

Factorization and dispersion relations for radiative leptonic B decay

Yu-Ming Wang

*Fakultät für Physik, Universität Wien, Boltzmanngasse 5, 1090 Vienna, Austria
School of Physics, Nankai University, 300071 Tianjin, China*

Abstract

Applying the dispersion approach we compute perturbative QCD corrections to the power suppressed soft contribution of $B \rightarrow \gamma \ell \nu$ at leading twist. QCD factorization for the $B \rightarrow \gamma^*$ form factors is demonstrated explicitly for the hard-collinear transverse polarized photon at one loop, with the aid of the method of regions. While the one-loop hard function is identical to the matching coefficient of the QCD weak current $\bar{u} \gamma_{\mu\perp} (1 - \gamma_5) b$ in soft-collinear effective theory, the jet function from integrating out the hard-collinear fluctuations differs from the corresponding one entering the factorization formula of $B \rightarrow \gamma \ell \nu$, due to the appearance of an additional hard-collinear momentum mode. Furthermore, we evaluate the sub-leading power contribution to the $B \rightarrow \gamma$ form factors from the three-particle B -meson distribution amplitudes (DAs) at tree level, with the dispersion approach. The soft contribution to the $B \rightarrow \gamma$ form factors from the three-particle B -meson DAs is shown to be of the same power compared with the corresponding hard correction, in contrast to the two-particle counterparts. Numerically the next-to-leading-order QCD correction to the soft two-particle contribution in $B \rightarrow \gamma$ form factors will induce an approximately $(10 \sim 20)\%$ shift to the tree-level contribution at $\lambda_B(\mu_0) = 354 \text{ MeV}$. Albeit of power suppression parametrically, the soft two-particle correction can decrease the leading power predictions for the $B \rightarrow \gamma$ form factors by an amount of $(10 \sim 30)\%$ with the same value of $\lambda_B(\mu_0)$. Employing the phenomenological model of the three-particle B -meson DAs inspired by a QCD sum rule analysis, the three-particle contribution to the $B \rightarrow \gamma$ form factors is predicted to be of $\mathcal{O}(1\%)$, at leading order in α_s , with the default theory inputs. Finally, we explore theory constraints on the inverse moment of the leading-twist B -meson DA λ_B from the recent Belle measurements of the partial branching fractions of $B \rightarrow \gamma \ell \nu$, taking into account the newly computed contributions to the $B \rightarrow \gamma$ form factors at subleading power.

1 Introduction

The radiative leptonic $B \rightarrow \gamma \ell \nu$ decay serves as one of the benchmark channels to understand the strong interaction dynamics of the B -meson system based upon the heavy quark expansion. Factorization properties of the $B \rightarrow \gamma \ell \nu$ amplitude at large photon energy E_γ have been explored extensively in both QCD [1, 2] and soft-collinear effective theory [3, 4] at leading power in Λ/E_γ . The particular feature of this channel lies in the strong sensitivity of the branching fraction $\mathcal{BR}(B \rightarrow \gamma \ell \nu)$ on the inverse moment λ_B of the B -meson light-cone distribution amplitude (DA) $\phi_B^+(\omega, \mu)$, which also enters the QCD factorization formulae for hadronic B -meson decays. Improving the theory description of the radiative leptonic $B \rightarrow \gamma \ell \nu$ decay by taking into account the subleading power effects is therefore in demand to achieve a better control over the inverse moment λ_B .

Subleading power corrections to $B \rightarrow \gamma \ell \nu$ in the heavy quark expansion were investigated in QCD factorization at tree level [5] where a symmetry-conserving form factor $\xi(E_\gamma)$ was introduced to parameterize the non-local power correction. It remains unclear whether $\xi(E_\gamma)$ can be computed straightforwardly in QCD factorization without encountering rapidity divergences. An alternative approach to evaluate the power suppressed contributions in $B \rightarrow \gamma \ell \nu$ was proposed in [6] by employing the dispersion relations and quark-hadron duality, where the “soft” two-particle correction to the $B \rightarrow \gamma$ form factors was computed at leading order in the perturbative expansion. The main purpose of this paper is to extend the calculation performed in [6] by computing the subleading power contributions to the $B \rightarrow \gamma \ell \nu$ amplitude from the two-particle DA $\phi_B^+(\omega, \mu)$ at one loop and from the three-particle DAs at tree level, for the sake of understanding the factorization properties of the higher power terms in the heavy quark expansion.

The basic idea of the dispersion approach is to first construct the sum rules for the generalized form factors of $B \rightarrow \gamma^* \ell \nu$ involving a spacelike hard-collinear photon with momentum p , and to perform the analytical continuation to $p^2 = 0$ to obtain the expressions for the on-shell $B \rightarrow \gamma$ form factors due to absence of the massless vector resonances. The primary task of evaluating the two-particle contribution to the above-mentioned sum rules at next-to-leading order in α_s is to demonstrate QCD factorization for the $B \rightarrow \gamma^*$ form factors, which can be achieved with either the soft-collinear effective theory (SCET) technique [7–9] or the diagrammatic approach based upon the method of regions [10]. We will, following [11, 12], adopt the latter approach to establish the factorization formula for the leading-twist contribution to $\mathcal{A}(B \rightarrow \gamma^* \ell \nu)$ at one loop and employ the renormalization-group (RG) approach to resum large logarithms in the perturbative functions at next-to-leading-logarithmic (NLL) accuracy. It is evident that the hard function entering the factorization formula of $\mathcal{A}(B \rightarrow \gamma^* \ell \nu)$ with a (transversely polarized) hard-collinear photon can be extracted directly from the perturbative matching coefficient of the QCD weak current $\bar{u} \gamma_{\mu\perp} (1 - \gamma_5) b$ in SCET, due to the absence of an additional hard-momentum mode; and in the limit $p^2 = 0$ the resulting hard-collinear function must reproduce the jet function in the SCET factorization for the $B \rightarrow \gamma \ell \nu$ decay amplitude. Applying the light-cone expansion for the massless quark propagator in the background gluon field, we will demonstrate that QCD factorization for the three-particle contribution to $\mathcal{A}(B \rightarrow \gamma \ell \nu)$ is already violated at tree level due to the emergence of end-point divergences, and the dispersion approach developed in [6] provides a coherent framework to

calculate the subleading power contributions from both the leading and higher Fock states of the B -meson. Following the established power counting scheme, we further show that both the “hard” and “soft” effects from the three-particle B -meson DAs contribute to the sum rules at the same power in Λ/m_b , in contrast to the observation for the leading twist contribution.

Yet another approach to address the subleading power contributions to the $B \rightarrow \gamma \ell \nu$ amplitude from the photon emission at large distance is to introduce the photon DAs describing the strong interaction dynamics for the “hadronic” component of a collinear real photon. Employing the vacuum-to-photon correlation function with the B -meson replaced by a local pseudoscalar current, the leading-twist contribution of such long-distance photon effect has been computed from QCD light-cone sum rules (LCSR) at tree level [13, 14] and at one loop [15]. Interestingly, the higher-twist correction to the hadronic photon contribution calculated in the same framework was found to violate the symmetry relation for two $B \rightarrow \gamma$ form factors due to the helicity conservation in the heavy quark limit [15]. Computing the hadronic photon effect in $\mathcal{A}(B \rightarrow \gamma \ell \nu)$ from QCD factorization with the photon DAs would be of great interest to develop a better understanding towards the pattern of the subleading power contributions from different dynamical sources. However, it is quite conceivable that the convolution integral involving the B -meson and photon DAs suffers from the end-point divergences, indicated from a direct calculation of the similar effect on the $\pi \rightarrow \gamma$ form factor [16].

The presentation is structured as follows. In Section 2 we will discuss some general aspects of the $B \rightarrow \gamma \ell \nu$ amplitude and summarize the main idea of computing the (soft) end-point contributions to the $B \rightarrow \gamma$ form factors in the dispersion approach, by working out the tree-level sum rules for the power suppressed two-particle contribution. We then demonstrate QCD factorization for the leading twist contribution to the generalized $B \rightarrow \gamma^* \ell \nu$ form factors at $\mathcal{O}(\alpha_s)$ with the diagrammatical factorization approach in Section 3, where the sum rules for the two-particle subleading power contribution to $\mathcal{A}(B \rightarrow \gamma \ell \nu)$ are also derived at NLL accuracy. We further compute the subleading power three-particle contribution to the $B \rightarrow \gamma$ form factors from the dispersion approach at tree level in Section 4, which constitutes another new result of this paper. Phenomenological implications of the newly computed contributions to the $B \rightarrow \gamma \ell \nu$ amplitude are explored in Section 5, including the uncertainty estimates for our predictions from different dynamical sources. Section 6 is reserved for a summary of main observations and concluding discussions.

2 The radiative leptonic $B \rightarrow \gamma \ell \nu$ decay in dispersion approach

2.1 General aspects of the $B \rightarrow \gamma \ell \nu$ amplitude

We will follow closely the theory overview of $B \rightarrow \gamma \ell \nu$ presented in [5] and the corresponding decay amplitude can be written as

$$\mathcal{A}(B^- \rightarrow \gamma \ell \nu) = \frac{G_F V_{ub}}{\sqrt{2}} \langle \gamma(p) \ell(p_\ell) \nu(p_\nu) | [\bar{\ell} \gamma_\mu (1 - \gamma_5) \nu] [\bar{u} \gamma^\mu (1 - \gamma_5) b] | B^-(p+q) \rangle, \quad (1)$$

where $p + q$ and p denote the momenta of the B -meson and photon, and the lepton-pair momentum is given by $q = p_\ell + p_\nu$ with p_ℓ and p_ν being the lepton and neutrino momenta, respectively. We will work in the rest frame of the B -meson with the velocity vector $v^\mu = (p^\mu + q^\mu)/m_B$ and introduce two light-cone vectors n_μ and \bar{n}_μ by defining

$$p_\mu = \frac{n \cdot p}{2} \bar{n}_\mu \equiv E_\gamma \bar{n}_\mu, \quad q_\mu = \frac{n \cdot q}{2} \bar{n}_\mu + \frac{\bar{n} \cdot q}{2} n_\mu, \quad v_\mu = \frac{n_\mu + \bar{n}_\mu}{2}. \quad (2)$$

Computing the amplitude $\mathcal{A}(B^- \rightarrow \gamma \ell \nu)$ in (1) to the first order in the electromagnetic interaction yields

$$\mathcal{A}(B^- \rightarrow \gamma \ell \nu) = \frac{G_F V_{ub}}{\sqrt{2}} (i g_{em} \epsilon_\nu^*) \left\{ T^{\nu\mu}(p, q) \bar{\ell} \gamma_\mu (1 - \gamma_5) \nu + Q_\ell f_B \bar{\ell} \gamma^\nu (1 - \gamma_5) \nu \right\}, \quad (3)$$

where the two terms in the bracket correspond to the photon emission from the partonic constituents of the B -meson and from the final-state lepton. The hadronic tensor $T^{\nu\mu}(p, q)$ is defined by the following non-local matrix element

$$T_{\nu\mu}(p, q) \equiv \int d^4x e^{ip \cdot x} \langle 0 | T \{ j_{\nu, \text{em}}(x), [\bar{u} \gamma_\mu (1 - \gamma_5) b](0) \} | B^-(p + q) \rangle, \quad (4)$$

where we adopt the convention for the QCD and QED covariant derivative $iD_\mu = i\partial_\mu + g_{\text{em}} Q_f A_{\mu, \text{em}} + g_s T^a A_\mu^a$ with $Q_f = -1$ for the lepton fields, and the electromagnetic current is given by $j_{\nu, \text{em}} = \sum_q Q_q \bar{q} \gamma_\nu q + Q_\ell \bar{\ell} \gamma_\nu \ell$. It is straightforward to write down the general decomposition of this hadronic matrix element [17, 18]

$$\begin{aligned} T_{\nu\mu}(p, q) = & v \cdot p \left[-i \epsilon_{\mu\nu\rho\sigma} n^\rho v^\sigma F_V(n \cdot p) + g_{\mu\nu} \hat{F}_A(n \cdot p) \right] + v_\nu p_\mu F_1(n \cdot p) \\ & + v_\mu p_\nu F_2(n \cdot p) + v \cdot p v_\mu v_\nu F_3(n \cdot p) + \frac{p_\mu p_\nu}{v \cdot p} F_4(n \cdot p), \end{aligned} \quad (5)$$

with the convention $\epsilon^{0123} = +1$. It is evident that the form factors $F_2(n \cdot p)$ and $F_4(n \cdot p)$ will not contribute to the amplitude $\mathcal{A}(B^- \rightarrow \gamma \ell \nu)$ in virtue of $\epsilon^* \cdot p = 0$. Employing the Ward identity $p_\nu T^{\nu\mu}(p, q) = -(Q_b - Q_u) f_B p_B^\mu$ due to the conservation of the vector current, we can further obtain

$$\hat{F}_A(n \cdot p) = -F_1(n \cdot p), \quad F_3(n \cdot p) = -\frac{(Q_b - Q_u) f_B m_B}{(v \cdot p)^2}. \quad (6)$$

Since the real photon is transversely polarized, the form factor $F_3(v \cdot p)$ will play no role in the $B \rightarrow \gamma \ell \nu$ amplitude. Finally, one can redefine the axial form factor $\hat{F}_A(v \cdot p)$ [5]

$$\begin{aligned} T_{\nu\mu}(p, q) \rightarrow & -i v \cdot p \epsilon_{\mu\nu\rho\sigma} n^\rho v^\sigma F_V(n \cdot p) + [g_{\mu\nu} v \cdot p - v_\nu p_\mu] \underbrace{\left[\hat{F}_A(n \cdot p) + \frac{Q_\ell f_B}{v \cdot p} \right]}_{\equiv F_A(n \cdot p)} \\ & - Q_\ell f_B g_{\mu\nu}, \end{aligned} \quad (7)$$

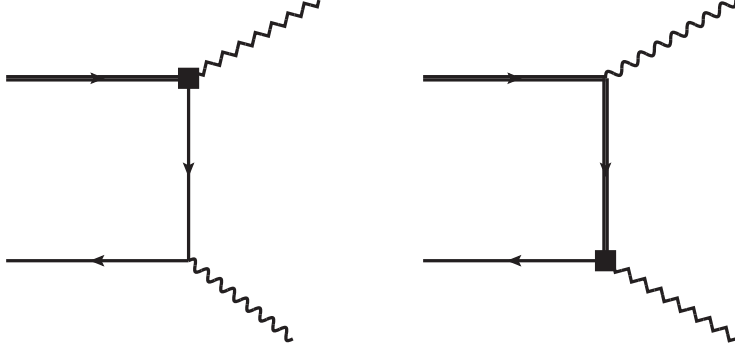


Figure 1: Diagrammatical representation of the correlation function (9) at tree level. The square boxes refer to insertions of the weak vertex “ $\bar{u}\gamma_{\mu\perp}(1-\gamma_5)b$ ” and the wavelines indicate photon radiations off the partons inside the B -meson.

where the last term cancels precisely the second term in the bracket of (3) due to the photon radiation off the lepton. The differential decay rate of $B \rightarrow \gamma\ell\nu$ in the B -meson rest frame can be readily computed as

$$\frac{d\Gamma}{dE_\gamma}(B \rightarrow \gamma\ell\nu) = \frac{\alpha_{em}^2 G_F^2 |V_{ub}|^2}{6\pi^2} m_B E_\gamma^3 \left(1 - \frac{2E_\gamma}{m_B}\right) [F_V^2(n \cdot p) + F_A^2(n \cdot p)] . \quad (8)$$

Evaluating the partial branching fractions of $B \rightarrow \gamma\ell\nu$ with an energetic photon is then traded to the QCD calculation of the two $B \rightarrow \gamma$ form factors.

2.2 Dispersion relations for the $B \rightarrow \gamma$ form factors

The aim of this subsection is to discuss the essential strategies for calculating the $B \rightarrow \gamma$ form factors from the dispersion approach which is originally proposed in [19] for the computation of the $\gamma^*\pi \rightarrow \gamma$ form factor with large momentum transfer (see also [16] for an updated analysis including the higher-twist corrections). Following [6] we start with construction of the correlation function

$$\begin{aligned} \tilde{T}_{\nu\mu}(p, q) &\equiv \int d^4x e^{ip \cdot x} \langle 0 | T \{ j_{\nu,em}^\perp(x), [\bar{u}\gamma_{\mu\perp}(1-\gamma_5)b](0) \} | B^-(p+q) \rangle \Big|_{p^2 < 0} , \\ &= v \cdot p \left[-i \epsilon_{\mu\nu\rho\sigma} n^\rho v^\sigma F_V^{B \rightarrow \gamma^*}(n \cdot p, \bar{n} \cdot p) + g_{\mu\nu}^\perp \hat{F}_A^{B \rightarrow \gamma^*}(n \cdot p, \bar{n} \cdot p) \right] , \end{aligned} \quad (9)$$

describing the $B \rightarrow \gamma^*\ell\nu$ transition with a (transversely polarized) hard-collinear photon. For definiteness, we work with the following power counting scheme

$$n \cdot p \sim \mathcal{O}(m_b), \quad |\bar{n} \cdot p| \sim \mathcal{O}(\Lambda). \quad (10)$$

At tree level we need to evaluate the two diagrams displayed in figure 1 with (light-cone) operator product expansion (OPE). It is apparent that photon emission off the heavy b -quark will only induce the subleading power contribution based upon the power counting

analysis. The resulting local effect independent of the soft momentum $\bar{n} \cdot p$ is identical to the corresponding result presented in [5], however, the non-local subleading power correction at tree level differs from the symmetry-conserving form factor $\xi(E_\gamma)$ discussed in the context of the $B \rightarrow \gamma \ell \nu$ transition. In this paper we will take the Born result of the local subleading power contribution to $\tilde{T}_{\nu\mu}(p, q)$ from [5] directly

$$F_{V,NLP}^{\text{LC}}(n \cdot p) = -\hat{F}_{A,NLP}^{\text{LC}}(n \cdot p) = \frac{Q_u f_B m_B}{(n \cdot p)^2} + \frac{Q_b f_B m_B}{n \cdot p m_b}, \quad (11)$$

and leave out the non-local power correction which could be expressed in terms of the higher-twist B -meson DAs.

Computing the leading power contribution from photon radiation off the up anti-quark at tree level yields

$$\begin{aligned} F_{V,2P}^{B \rightarrow \gamma^*}(n \cdot p, \bar{n} \cdot p) &= \hat{F}_{A,2P}^{B \rightarrow \gamma^*}(n \cdot p, \bar{n} \cdot p) \\ &= \frac{Q_u \tilde{f}_B(\mu) m_B}{n \cdot p} \int_0^\infty d\omega \frac{\phi_B^+(\omega, \mu)}{\omega - \bar{n} \cdot p - i0} + \mathcal{O}(\alpha_s, \Lambda/m_b), \end{aligned} \quad (12)$$

where the B -meson DA $\phi_B^+(\omega, \mu)$ is defined as [20–22]

$$i \tilde{f}_B(\mu) m_B \phi_B^+(\omega, \mu) = \frac{1}{2\pi} \int_0^\infty dt e^{i\omega t} \langle 0 | (\bar{q}_s Y_s)(t \bar{n}) \not{n} \gamma_5 (Y_s^\dagger b_v)(0) | \bar{B}(v) \rangle, \quad (13)$$

with the soft Wilson link

$$Y_s(t \bar{n}) = \text{P} \left\{ \text{Exp} \left[i g_s \int_{-\infty}^t dx \bar{n} \cdot A_s(x \bar{n}) \right] \right\}. \quad (14)$$

At one loop, the HQET decay constant $\tilde{f}_B(\mu)$ of the B -meson can be expressed in terms of the QCD decay constant f_B as follows

$$\tilde{f}_B(\mu) = \left\{ 1 + \frac{\alpha_s(\mu) C_F}{4\pi} \left[3 \ln \frac{m_b}{\mu} - 2 \right] \right\}^{-1} f_B. \quad (15)$$

Taking into account the fact that $F_V^{B \rightarrow \gamma^*}$ and $\hat{F}_A^{B \rightarrow \gamma^*}$ are analytical functions in the variable p^2 (or $\bar{n} \cdot p$ equivalently), we can derive the following hadronic dispersion relations

$$\begin{aligned} F_V^{B \rightarrow \gamma^*}(n \cdot p, \bar{n} \cdot p) &= \frac{2}{3} \frac{f_\rho m_\rho}{m_\rho^2 - p^2 - i0} \frac{2 m_B}{m_B + m_\rho} V(q^2) \\ &\quad + \frac{1}{\pi} \int_{\omega_s}^\infty d\omega' \frac{\text{Im}_{\omega'} F_V^{B \rightarrow \gamma^*, \text{had}}(n \cdot p, \omega')}{\omega' - \bar{n} \cdot p - i0}, \end{aligned} \quad (16)$$

$$\begin{aligned} \hat{F}_A^{B \rightarrow \gamma^*}(n \cdot p, \bar{n} \cdot p) &= \frac{2}{3} \frac{f_\rho m_\rho}{m_\rho^2 - p^2 - i0} \frac{2(m_B + m_\rho)}{n \cdot p} A_1(q^2) \\ &\quad + \frac{1}{\pi} \int_{\omega_s}^\infty d\omega' \frac{\text{Im}_{\omega'} \hat{F}_A^{B \rightarrow \gamma^*, \text{had}}(n \cdot p, \omega')}{\omega' - \bar{n} \cdot p - i0}, \end{aligned} \quad (17)$$

where the ground-state contributions from ρ and ω are combined into one resonance term with the narrow-width approximation and with the assumption $m_\rho \simeq m_\omega$. The relevant $B \rightarrow \rho$ form factors are defined as

$$\begin{aligned} \sqrt{2} \langle \rho^0(p) | \bar{u} \gamma_\mu (1 - \gamma_5) b | B^-(p+q) \rangle &= -\epsilon_{\mu\nu\rho\sigma} \epsilon_V^{*\nu} q^\rho p^\sigma \frac{2V(q^2)}{m_B + m_\rho} - i \epsilon_V^*{}_\mu (m_B + m_\rho) A_1(q^2) \\ &+ i (2p + q)_\mu (\epsilon_V^* \cdot q) \frac{A_2(q^2)}{m_B + m_\rho} - i q_\mu (\epsilon_V^* \cdot q) \frac{2m_\rho}{q^2} [A_3(q^2) - A_0(q^2)] , \end{aligned} \quad (18)$$

where ϵ_V is the polarization vector of the ρ meson. Applying the parton-hadron duality approximation and performing the Borel transformation with respect to the variable $\bar{n} \cdot p$ yields the sum rules for the $B \rightarrow \rho$ form factors $V(q^2)$ and $A_1(q^2)$

$$\frac{2}{3} \frac{f_\rho m_\rho}{n \cdot p} \text{Exp} \left[-\frac{m_\rho^2}{n \cdot p \omega_M} \right] \frac{2m_B}{m_B + m_\rho} V(q^2) = \frac{1}{\pi} \int_0^{\omega_s} d\omega' e^{-\omega'/\omega_M} \text{Im}_{\omega'} F_V^{B \rightarrow \gamma^*}(n \cdot p, \omega') , \quad (19)$$

$$\frac{2}{3} \frac{f_\rho m_\rho}{n \cdot p} \text{Exp} \left[-\frac{m_\rho^2}{n \cdot p \omega_M} \right] \frac{2(m_B + m_\rho)}{n \cdot p} A_1(q^2) = \frac{1}{\pi} \int_0^{\omega_s} d\omega' e^{-\omega'/\omega_M} \text{Im}_{\omega'} \hat{F}_A^{B \rightarrow \gamma^*}(n \cdot p, \omega') , \quad (20)$$

where the QCD spectral functions at tree level can be readily extracted from (12)

$$\begin{aligned} \frac{1}{\pi} \text{Im}_{\omega'} F_V^{B \rightarrow \gamma^*}(n \cdot p, \omega') &= \frac{1}{\pi} \text{Im}_{\omega'} \hat{F}_A^{B \rightarrow \gamma^*}(n \cdot p, \omega') \\ &= \frac{Q_u \tilde{f}_B(\mu) m_B}{n \cdot p} \phi_B^+(\omega', \mu) + \mathcal{O}(\alpha_s, \Lambda/m_b) . \end{aligned} \quad (21)$$

Substituting the resulting LCSR (19) and (20) into the dispersion relations (16) and (17) and setting $\bar{n} \cdot p \rightarrow 0$, we obtain the final expressions for the on-shell $B \rightarrow \gamma$ form factors

$$\begin{aligned} F_V(n \cdot p) &= \frac{1}{\pi} \int_0^{\omega_s} d\omega' \frac{n \cdot p}{m_\rho^2} \text{Exp} \left[\frac{m_\rho^2 - \omega' n \cdot p}{n \cdot p \omega_M} \right] \left[\text{Im}_{\omega'} F_V^{B \rightarrow \gamma^*}(n \cdot p, \omega') \right] \\ &+ \frac{1}{\pi} \int_{\omega_s}^\infty d\omega' \frac{1}{\omega'} \left[\text{Im}_{\omega'} F_V^{B \rightarrow \gamma^*}(n \cdot p, \omega') \right] , \end{aligned} \quad (22)$$

$$\begin{aligned} \hat{F}_A(n \cdot p) &= \frac{1}{\pi} \int_0^{\omega_s} d\omega' \frac{n \cdot p}{m_\rho^2} \text{Exp} \left[\frac{m_\rho^2 - \omega' n \cdot p}{n \cdot p \omega_M} \right] \left[\text{Im}_{\omega'} \hat{F}_A^{B \rightarrow \gamma^*}(n \cdot p, \omega') \right] \\ &+ \frac{1}{\pi} \int_{\omega_s}^\infty d\omega' \frac{1}{\omega'} \left[\text{Im}_{\omega'} \hat{F}_A^{B \rightarrow \gamma^*}(n \cdot p, \omega') \right] , \end{aligned} \quad (23)$$

where two nonperturbative parameters ω_s and m_ρ are introduced, as compared to the direct QCD calculation, to avoid the evaluation of the “hadronic” photon contribution. To develop a better understanding of the master formulae (22) and (23) for the form factors $F_V(n \cdot p)$ and $\hat{F}_A(n \cdot p)$, one can rewrite these expressions as follows

$$F_V(n \cdot p) = \frac{1}{\pi} \int_0^\infty d\omega' \frac{1}{\omega'} \left[\text{Im}_{\omega'} F_V^{B \rightarrow \gamma^*}(n \cdot p, \omega') \right]$$

$$+\frac{1}{\pi} \int_0^{\omega_s} d\omega' \left\{ \frac{n \cdot p}{m_\rho^2} \text{Exp} \left[\frac{m_\rho^2 - \omega' n \cdot p}{n \cdot p \omega_M} \right] - \frac{1}{\omega'} \right\} \left[\text{Im}_{\omega'} F_V^{B \rightarrow \gamma^*}(n \cdot p, \omega') \right], \quad (24)$$

$$\begin{aligned} \hat{F}_A(n \cdot p) &= \frac{1}{\pi} \int_0^\infty d\omega' \frac{1}{\omega'} \left[\text{Im}_{\omega'} \hat{F}_A^{B \rightarrow \gamma^*}(n \cdot p, \omega') \right] \\ &+ \frac{1}{\pi} \int_0^{\omega_s} d\omega' \left\{ \frac{n \cdot p}{m_\rho^2} \text{Exp} \left[\frac{m_\rho^2 - \omega' n \cdot p}{n \cdot p \omega_M} \right] - \frac{1}{\omega'} \right\} \left[\text{Im}_{\omega'} \hat{F}_A^{B \rightarrow \gamma^*}(n \cdot p, \omega') \right]. \quad (25) \end{aligned}$$

It is evident that the first term on the right-hand side of (24) and (25) is precisely the expression obtained from the QCD factorization approach, provided that the convolution integrals of the B -meson DAs with the perturbatively calculable functions are free of rapidity divergences. In accordance with the power counting rule

$$\omega_s \sim \omega_M \sim \mathcal{O}(\Lambda^2/m_b), \quad (26)$$

we observe that the second term on the right-hand side of (24) and (25) can be identified as the nonperturbative modification of the spectral function in the end-point region. Exploring the canonical behaviour of the B -meson DA $\phi_B^+(\omega, \mu)$ and employing the tree-level expressions of the QCD spectral functions (12) one can readily verify that the end-point contributions to the $B \rightarrow \gamma$ form factors are indeed suppressed by a factor of Λ/m_b compared to the effects computed from the direct QCD approach.

3 Two-particle subleading power contribution at $\mathcal{O}(\alpha_s)$

The objective of this section is to compute the one-loop corrections to the perturbative hard and jet functions entering the factorization formulae of the generalized form factors for the $B \rightarrow \gamma^* \ell \nu$ transition

$$\begin{aligned} F_V^{B \rightarrow \gamma^*}(n \cdot p, \bar{n} \cdot p) &= \hat{F}_A^{B \rightarrow \gamma^*}(n \cdot p, \bar{n} \cdot p) \\ &= \frac{Q_u \tilde{f}_B(\mu) m_B}{n \cdot p} C_\perp(n \cdot p, \mu) \int_0^\infty d\omega \frac{\phi_B^+(\omega, \mu)}{\omega - \bar{n} \cdot p - i0} J_\perp(n \cdot p, \bar{n} \cdot p, \omega, \mu) + \dots, \quad (27) \end{aligned}$$

at leading power in Λ/m_b , where the ellipses represent the subleading power terms. As mentioned in the Introduction, we will extract the hard coefficient function (C_\perp) and the jet function J_\perp simultaneously by performing the perturbative matching at the diagrammatic level with the aid of the method of regions, and demonstrate the factorization-scale independence of the form factors $F_V^{B \rightarrow \gamma^*}$ and $\hat{F}_A^{B \rightarrow \gamma^*}$ explicitly at one loop by exploiting the RG equations of both the short-distance functions and the B -meson DA $\phi_B^+(\omega, \mu)$. Now we will, following the presentation of [11] closely, evaluate the one-loop QCD diagrams for the correlation function (9) displayed figure 2 in detail.

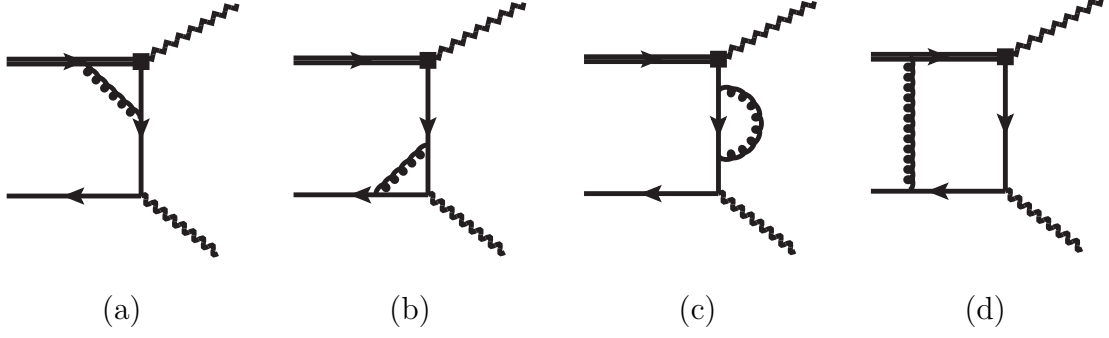


Figure 2: QCD corrections to the correlation function (9) at one loop. Same conventions as in figure 1.

3.1 Weak vertex diagram

The one-loop correction to the weak vertex diagram displayed in figure 2(a) can be readily computed as

$$\begin{aligned} \tilde{T}_{\nu\mu,weak}^{(1)}(p, q) &= \frac{Q_u g_s^2 C_F}{\bar{n} \cdot p - \omega} \int \frac{d^D l}{(2\pi)^D} \frac{1}{[(p - k + l)^2 + i0] [(m_b v + l)^2 - m_b^2 + i0] [l^2 + i0]} \\ &\times \left\{ n \cdot l [(D - 2) \bar{n} \cdot l + 2 m_b] + (D - 4) l_\perp^2 + 2 n \cdot p (\bar{n} \cdot l + m_b) \right\} \\ &\times \bar{u}(k) \gamma_{\nu\perp} \frac{\not{l}}{2} \gamma_{\mu\perp} (1 - \gamma_5) b(v), \end{aligned} \quad (28)$$

where we adopt the following conventions

$$l_\perp^2 \equiv g_\perp^{\mu\nu} l_\mu l_\nu, \quad g_\perp^{\mu\nu} \equiv g^{\mu\nu} - \frac{n^\mu \bar{n}^\nu}{2} - \frac{n^\nu \bar{n}^\mu}{2}. \quad (29)$$

Applying the power counting rule for the external momenta

$$n \cdot p \sim \mathcal{O}(m_b), \quad \bar{n} \cdot p \sim \mathcal{O}(\Lambda), \quad k_\mu \sim \mathcal{O}(\Lambda), \quad (30)$$

it is straightforward to identify that the leading-power contributions of $\tilde{T}_{\nu\mu,weak}^{(1)}$ arise from the hard, hard-collinear and soft regions of the loop momentum.

Evaluating the leading power hard contribution from the weak vertex diagram with the method of regions yields

$$\begin{aligned} \tilde{T}_{\nu\mu,weak}^{(1),h}(p, q) &= -i g_s^2 C_F \int \frac{d^D l}{(2\pi)^D} \frac{\tilde{T}_{\nu\mu}^{(0)}(p, q)}{[l^2 + n \cdot p \bar{n} \cdot l + i0] [l^2 + 2 m_b v \cdot l + i0] [l^2 + i0]} \\ &\times \left\{ n \cdot l [(D - 2) \bar{n} \cdot l + 2 m_b] + (D - 4) l_\perp^2 + 2 n \cdot p (\bar{n} \cdot l + m_b) \right\} \\ &\equiv C_{\perp,weak}(n \cdot p) \tilde{T}_{\nu\mu}^{(0)}(p, q), \end{aligned} \quad (31)$$

where $\tilde{T}_{\nu\mu}^{(0)}(p, q)$ is the leading order contribution to the correlation function (9)

$$\tilde{T}_{\nu\mu}^{(0)}(p, q) = \frac{i Q_u}{\bar{n} \cdot p - \omega} \bar{u}(k) \gamma_{\nu\perp} \frac{\not{n}}{2} \gamma_{\mu\perp} (1 - \gamma_5) b(v), \quad (32)$$

and the resulting hard function $C_{\perp, weak}(n \cdot p, \mu)$ is given by

$$C_{\perp, weak}(n \cdot p, \mu) = -\frac{\alpha_s C_F}{4\pi} \left[\frac{1}{\epsilon^2} + \frac{1}{\epsilon} \left(2 \ln \frac{\mu}{n \cdot p} + 1 \right) + 2 \ln^2 \frac{\mu}{n \cdot p} + 2 \ln \frac{\mu}{m_b} \right. \\ \left. - 2 \text{Li}_2 \left(1 - \frac{1}{r} \right) - \ln^2 r + \frac{3r-2}{1-r} \ln r + \frac{\pi^2}{12} + 4 \right], \quad (33)$$

with $r = n \cdot p / m_b$. It is evident that $C_{\perp, weak}(n \cdot p)$ is precisely the same as the hard contribution to the weak vertex diagram for the vacuum-to- Λ_b -baryon correlation function at one loop [12].

Proceeding in a similar manner, we can extract the hard-collinear correction from figure 2(a) by expanding (28) in the hard-collinear region

$$\tilde{T}_{\nu\mu, weak}^{(1), hc}(p, q) = -i g_s^2 C_F \int \frac{d^D l}{(2\pi)^D} \frac{2 m_b n \cdot (p + l) \tilde{T}_{\nu\mu}^{(0)}(p, q)}{[n \cdot (p + l) \bar{n} \cdot (p - k + l) + l_\perp^2 + i0][m_b n \cdot l + i0][l^2 + i0]} \\ \equiv J_{\perp, weak}(n \cdot p, \bar{n} \cdot p, \omega) \tilde{T}_{\nu\mu}^{(0)}(p, q), \quad (34)$$

where the perturbative jet function $J_{\perp, weak}(n \cdot p, \bar{n} \cdot p, \omega)$ at $\mathcal{O}(\alpha_s)$ reads

$$J_{\perp, weak}(n \cdot p, \bar{n} \cdot p, \omega, \mu) = \frac{\alpha_s C_F}{4\pi} \left[\frac{2}{\epsilon^2} + \frac{2}{\epsilon} \left(\ln \frac{\mu^2}{n \cdot p (\omega - \bar{n} \cdot p)} + 1 \right) + \ln^2 \frac{\mu^2}{n \cdot p (\omega - \bar{n} \cdot p)} \right. \\ \left. + 2 \ln \frac{\mu^2}{n \cdot p (\omega - \bar{n} \cdot p)} - \frac{\pi^2}{6} + 4 \right], \quad (35)$$

in agreement with [11]. Setting $\bar{n} \cdot p \rightarrow 0$, our result of $J_{\perp, weak}$ reproduces the hard-collinear contribution to the weak vertex diagram in the $B \rightarrow \gamma \ell \nu$ decay (see (69) in [2]).

Furthermore, expanding the full QCD amplitude of $\tilde{T}_{\nu\mu, weak}^{(1)}(p, q)$ in the soft region at leading power leads to the soft contribution

$$\tilde{T}_{\nu\mu, weak}^{(1), s}(p, q) = -i g_s^2 C_F \int \frac{d^D l}{(2\pi)^D} \frac{1}{[\bar{n} \cdot (p - k + l) + i0][v \cdot l + i0][l^2 + i0]} \tilde{T}_{\nu\mu}^{(0)}(p, q), \quad (36)$$

which cancels precisely the soft subtraction term defined by the convolution integral of the two-particle B -meson DA $\phi_B^+(\omega, \mu)$ at $\mathcal{O}(\alpha_s)$ with the tree-level hard scattering kernel. One then concludes that soft dynamics of the weak vertex diagram in figure 2(a) can indeed be parametrized by the B -meson DAs in the framework of perturbative QCD.

3.2 Electromagnetic vertex diagram

We proceed to compute the one-loop correction to the electromagnetic vertex diagram shown in figure 2(b)

$$\tilde{T}_{\nu\mu, em}^{(1)}(p, q) = \frac{Q_u g_s^2 C_F}{n \cdot p (\omega - \bar{n} \cdot p)} \int \frac{d^D l}{(2\pi)^D} \frac{1}{[l^2 + i0][(p - l)^2 + i0][(l - k)^2 + i0]}$$

$$\bar{u}(k) \gamma_\rho \not{\ell} \gamma_\nu^\perp (\not{p} - \not{\ell}) \gamma^\rho (\not{p} - \not{k}) \gamma_\mu^\perp (1 - \gamma_5) b(v). \quad (37)$$

Employing the power counting rule (30) one can verify that only the hard-collinear and soft regions in (37) can give rise to the leading power contributions. Following the arguments of computing the pion vertex diagram for the vacuum-to- B -meson correlation function [11], it is more transparent to compute the loop integrals in (37) directly instead of employing the method of regions, and then to expand the resulting expression to the leading power in Λ/m_b . Evaluating the loop integral with the expressions collected in Appendix A of [11] yields

$$\begin{aligned} \tilde{T}_{\nu\mu,\text{em}}^{(1)}(p, q) &= \frac{\alpha_s C_F}{4\pi} \left\{ \frac{1}{\epsilon} \left[\frac{2}{\eta} \ln(1 + \eta) - 1 \right] + \frac{\ln(1 + \eta)}{\eta} \left[2 \ln \frac{\mu^2}{-p^2} - \ln(1 + \eta) + 3 \right] \right. \\ &\quad \left. - \ln \frac{\mu^2}{n \cdot p (\omega - \bar{n} \cdot p)} - 4 \right\} \tilde{T}_{\nu\mu}^{(0)}(p, q) \\ &\equiv J_{\perp,\text{em}}(n \cdot p, \bar{n} \cdot p, \omega, \mu) \tilde{T}_{\nu\mu}^{(0)}(p, q), \end{aligned} \quad (38)$$

with $\eta = -\omega/\bar{n} \cdot p$. It is straightforward to confirm that the obtained jet function $J_{\perp,\text{em}}$ can reproduce the hard-collinear correction to the electromagnetic vertex diagram in $B \rightarrow \gamma \ell \nu$ (see (33) in [2] and (A.5) in [3]) in the limit $\bar{n} \cdot p \rightarrow 0$, taking into account the fact that the soft contribution to $\tilde{T}_{\nu\mu,\text{em}}^{(1)}(p, q)$ vanishes in dimensional regularization. Following [11] one can further verify that the soft contribution from the electromagnetic vertex diagram cancels precisely the corresponding soft subtraction term, independent of the regularization scheme.

3.3 Wave function renormalization

The contribution from the wave function renormalization of the immediate quark propagator in figure 2(c) can be readily computed as

$$\begin{aligned} \tilde{T}_{\nu\mu,wfc}^{(1)}(p, q) &= -\frac{\alpha_s C_F}{4\pi} \left[\frac{1}{\epsilon} + \ln \frac{\mu^2}{n \cdot p (\omega - \bar{n} \cdot p)} + 1 \right] \tilde{T}_{\nu\mu}^{(0)}(p, q) \\ &\equiv J_{\perp,wfc}(n \cdot p, \bar{n} \cdot p, \omega, \mu) \tilde{T}_{\nu\mu}^{(0)}(p, q), \end{aligned} \quad (39)$$

which is apparently free of soft and collinear divergences. Evaluating the perturbative matching coefficients from the wave function renormalization of the external quark fields yields

$$\begin{aligned} \tilde{T}_{\nu\mu,bwf}^{(1)}(p, q) - \Phi_{b\bar{u},bwf}^{(1)} \otimes \tilde{T}_{\nu\mu}^{(0)}(p, q) &= -\frac{\alpha_s C_F}{8\pi} \left[\frac{3}{\epsilon} + 3 \ln \frac{\mu^2}{m_b^2} + 4 \right] \tilde{T}_{\nu\mu}^{(0)}(p, q) \\ &\equiv C_{\perp,bwf}(n \cdot p, \mu) \tilde{T}_{\nu\mu}^{(0)}(p, q), \end{aligned} \quad (40)$$

$$\tilde{T}_{\nu\mu,uf}^{(1)}(p, q) - \Phi_{b\bar{u},uf}^{(1)} \otimes \tilde{T}_{\nu\mu}^{(0)}(p, q) = 0, \quad (41)$$

where $\Phi_{b\bar{u}}$ is the partonic DA of the B -meson defined in (12) of [11].

3.4 Box diagram

Now we turn to compute the one-loop contribution to $\tilde{T}_{\nu\mu}^{(1)}(p, q)$ from the box diagram shown in figure 2(d)

$$\Pi_{\mu, box}^{(1)} = -Q_u g_s^2 C_F \int \frac{d^D l}{(2\pi)^D} \frac{1}{[(m_b v + l)^2 - m_b^2 + i0][(p - k + l)^2 + i0][(k - l)^2 + i0][l^2 + i0]} \bar{u}(k) \gamma_\rho (\not{k} - \not{l}) \gamma_{\nu\perp} (\not{p} - \not{k} + \not{l}) \gamma_{\mu\perp} (1 - \gamma_5) (m_b \not{p} + \not{l} + m_b) \gamma^\rho b(v). \quad (42)$$

As discussed in [2], this is the only one-loop diagram with no hard-collinear propagator outside of the loop, therefore the $1/(\omega - \bar{n} \cdot p)$ enhancement factor observed in the tree-level result (12) must come from singular regions of phase space in the loop integral. Based upon the power counting analysis, one can identify that the hard-collinear contribution to the following four-point scalar integral

$$I_{box} = \int \frac{d^D l}{(2\pi)^D} \frac{1}{[(m_b v + l)^2 - m_b^2 + i0][(p - k + l)^2 + i0][(k - l)^2 + i0][l^2 + i0]} \quad (43)$$

scales as λ^{-1} with the expansion parameter $\lambda = \Lambda/m_b$. The one-loop box diagram would then generate non-vanishing contribution to the jet function $J_\perp(n \cdot p, \bar{n} \cdot p, \omega, \mu)$ entering the factorization formula (1), provided that no additional suppression factor of λ can be induced from the Dirac algebra in (42). Inspecting the Dirac structure in the numerator of (42)

$$(\not{k} - \not{l}) \gamma_{\nu\perp} (\not{p} - \not{k} + \not{l})$$

shows that one cannot pick up the leading contributions of two hard-collinear propagators simultaneously in contrast to the case of the vacuum-to- B -meson correlation function as considered in [11]. Hence, one can conclude that no hard-collinear contribution can arise from the box diagram at one loop displayed in figure 2(d), confirming the observation made in [2].

Along the same vein, one can verify that the soft contribution to the scalar integral (43) scales as λ^{-2} and the Dirac algebra in (42) will again give rise to a suppression factor of λ in the soft region. It is then evident that the leading-power contribution to the box diagram comes only from the soft region at one loop, and following [11], such soft contribution will be cancelled precisely by the corresponding infrared subtraction term from the standard perturbative matching procedure.

3.5 Factorization of the two-particle contribution at $\mathcal{O}(\alpha_s)$

Collecting everything together, we can readily derive the renormalized hard and jet functions entering the factorization formula (27) for the generalized $B \rightarrow \gamma^*$ form factors at one loop

$$\begin{aligned} C_\perp &= 1 + C_{\perp, weak} + C_{\perp, bnf} \\ &= 1 - \frac{\alpha_s C_F}{4\pi} \left[2 \ln^2 \frac{\mu}{n \cdot p} + 5 \ln \frac{\mu}{m_b} - 2 \text{Li}_2 \left(1 - \frac{1}{r} \right) - \ln^2 r \right] \end{aligned}$$

$$+ \frac{3r-2}{1-r} \ln r + \frac{\pi^2}{12} + 6 \Big], \quad (44)$$

$$\begin{aligned} J_\perp &= 1 + J_{\perp,weak} + J_{\perp,em} + J_{\perp,wfc} \\ &= 1 + \frac{\alpha_s C_F}{4\pi} \left\{ \ln^2 \frac{\mu^2}{n \cdot p (\omega - \bar{n} \cdot p)} - \frac{\pi^2}{6} - 1 \right. \\ &\quad \left. - \frac{\bar{n} \cdot p}{\omega} \ln \frac{\bar{n} \cdot p - \omega}{\bar{n} \cdot p} \left[\ln \frac{\mu^2}{-p^2} + \ln \frac{\mu^2}{n \cdot p (\omega - \bar{n} \cdot p)} + 3 \right] \right\}. \end{aligned} \quad (45)$$

It is straightforward to verify that the hard function C_\perp coincides with the perturbative matching coefficient of the QCD weak current $\bar{u} \gamma_{\mu\perp} (1 - \gamma_5) b$ in SCET [23, 24]

$$\bar{u} \gamma_{\mu\perp} (1 - \gamma_5) b \rightarrow C_3(\mu) \bar{\xi}_{\bar{n}} W_{hc} \gamma_{\mu\perp} (1 - \gamma_5) Y_s^\dagger b_v + \dots, \quad (46)$$

where W_{hc} refers to the hard-collinear Wilson line and the ellipses represent the subleading power contributions.

We are now in a position to demonstrate the factorization-scale independence of the factorization formulae for $F_V^{B \rightarrow \gamma^*}$ and $\hat{F}_V^{B \rightarrow \gamma^*}$ explicitly at one loop. With the expressions for the hard and jet functions in (44) and (45), we obtain

$$\begin{aligned} \frac{d}{d \ln \mu} F_V^{B \rightarrow \gamma^*} &= \frac{d}{d \ln \mu} \hat{F}_V^{B \rightarrow \gamma^*} \\ &= \frac{Q_u \tilde{f}_B(\mu) m_B}{n \cdot p} \left\{ \int_0^\infty d\omega \frac{\phi_B^+(\omega, \mu)}{\omega - \bar{n} \cdot p - i0} \frac{\alpha_s C_F}{4\pi} \left[- \left(4 \ln \frac{\mu}{n \cdot p} + 5 \right) \right. \right. \\ &\quad \left. \left. + 4 \left(\ln \frac{\mu^2}{n \cdot p (\omega - \bar{n} \cdot p)} - \frac{\bar{n} \cdot p}{\omega} \ln \frac{\bar{n} \cdot p - \omega}{\bar{n} \cdot p} \right) + 3 \right] \right. \\ &\quad \left. + \int_0^\infty d\omega \frac{1}{\omega - \bar{n} \cdot p - i0} \frac{d}{d \ln \mu} \phi_B^+(\omega, \mu) \right\}, \end{aligned} \quad (47)$$

where the three terms in the square bracket appeared on the right-handed side of (47) correspond to the contributions from the scale evolutions of the hard and jet functions as well as the HQET decay constant of the B -meson, respectively. Employing the one-loop evolution equation of $\phi_B^+(\omega, \mu)$ [25, 26]

$$\frac{d\phi_B^+(\omega, \mu)}{d \ln \mu} = - \left[\Gamma_{\text{cusp}}(\alpha_s) \ln \frac{\mu}{\omega} + \gamma_+(\alpha_s) \right] \phi_B^+(\omega, \mu) - \omega \int_0^\infty d\omega' \Gamma_+(\omega, \omega', \mu) \phi_B^+(\omega', \mu) \quad (48)$$

with the anomalous dimensions

$$\begin{aligned} \Gamma_{\text{cusp}}(\alpha_s) &= \sum_{n=0} \left(\frac{\alpha_s}{4\pi} \right)^{n+1} \Gamma_{\text{cusp}}^{(n)}, & \Gamma_{\text{cusp}}^{(0)} &= 4 C_F, \\ \gamma_+(\alpha_s) &= \sum_{n=0} \left(\frac{\alpha_s}{4\pi} \right)^{n+1} \gamma_+^{(n)}, & \gamma_+^{(0)} &= -2 C_F, \end{aligned}$$

$$\Gamma_+(\omega, \omega', \mu) = -\frac{\alpha_s}{4\pi} \Gamma_{\text{cusp}}^{(0)} \left[\frac{\theta(\omega' - \omega)}{\omega'(\omega' - \omega)} + \frac{\theta(\omega - \omega')}{\omega(\omega - \omega')} \right]_{\oplus} + \mathcal{O}(\alpha_s^2), \quad (49)$$

the last term in the bracket of (47) can be further computed as

$$\begin{aligned} & \int_0^\infty d\omega \frac{1}{\omega - \bar{n} \cdot p - i0} \frac{d}{d \ln \mu} \phi_B^+(\omega, \mu) \\ &= \frac{\alpha_s C_F}{4\pi} \int_0^\infty d\omega \frac{\phi_B^+(\omega, \mu)}{\omega - \bar{n} \cdot p - i0} \left[4 \left(-\ln \frac{\mu}{\omega - \bar{n} \cdot p} + \frac{\bar{n} \cdot p}{\omega} \ln \frac{\bar{n} \cdot p - \omega}{\bar{n} \cdot p} \right) + 2 \right]. \end{aligned} \quad (50)$$

Here, the “ \oplus ”-function is defined in a standard way

$$\int_0^\infty d\omega [f(\omega, \omega')]_{\oplus} g(\omega) = \int_0^\infty d\omega f(\omega, \omega') [g(\omega) - g(\omega')]. \quad (51)$$

Substituting (50) into (47) leads us to conclude that the factorization-scale dependence indeed cancels out in the factorization formulae for the $B \rightarrow \gamma^*$ form factors at one loop, i.e.,

$$\frac{d}{d \ln \mu} F_V^{B \rightarrow \gamma^*} = \frac{d}{d \ln \mu} \hat{F}_A^{B \rightarrow \gamma^*} = \mathcal{O}(\alpha_s^2). \quad (52)$$

Now we turn to sum the parametrically large logarithms in perturbative matching coefficients to all orders at NLL by employing the standard RG approach in momentum space. Since the hard-collinear scale $\mu_{hc} \simeq \sqrt{\Lambda m_b}$ is comparable to the soft scale μ_0 entering the initial condition of the B -meson DA $\phi_B^+(\omega, \mu_0)$ for the actual value of the b -quark mass, we will not sum logarithms of μ_{hc}/μ_0 from the RG evolution of $\phi_B^+(\omega, \mu)$ when the factorization scale μ is taken as a hard-collinear scale as argued in [5]. Solving the evolution equations for the hard function C_\perp and the HQET decay constant f_B

$$\begin{aligned} \frac{dC_\perp(n \cdot p, \mu)}{d \ln \mu} &= \left[-\Gamma_{\text{cusp}}(\alpha_s) \ln \frac{\mu}{n \cdot p} + \gamma(\alpha_s) \right] C_\perp(n \cdot p, \mu), \\ \frac{d\tilde{f}_B(\mu)}{d \ln \mu} &= \tilde{\gamma}(\alpha_s) \tilde{f}_B(\mu), \end{aligned} \quad (53)$$

with the cusp anomalous dimension $\Gamma_{\text{cusp}}(\alpha_s)$ expanded up to three loops and the remaining anomalous dimensions $\gamma(\alpha_s)$ and $\tilde{\gamma}(\alpha_s)$ expanded up to the two-loop order, we then obtain the NLL resummation improved expressions for C_\perp and \tilde{f}_B

$$\begin{aligned} C_\perp(n \cdot p, \mu) &= U_1(n \cdot p, \mu_{h1}, \mu) C_\perp(n \cdot p, \mu_{h1}), \\ \tilde{f}_B(\mu) &= U_2(n \cdot p, \mu_{h2}, \mu) \tilde{f}_B(\mu_{h2}). \end{aligned} \quad (54)$$

The manifest expression of $U_1(n \cdot p, \mu_{h1}, \mu)$ can be deduced from $U_1(E_\gamma, \mu_{h1}, \mu)$ in [5] by replacing $E_\gamma \rightarrow n \cdot p/2$ and $U_2(n \cdot p, \mu_{h2}, \mu)$ can be read from $U_1(E_\gamma, \mu_{h1}, \mu)$ by setting the cusp anomalous dimension to zero and by replacing $\gamma^{(n)} \rightarrow \tilde{\gamma}^{(n)}$.

Finally we present the factorization formulae for the form factors $F_V^{B \rightarrow \gamma^*}$ and $\hat{F}_A^{B \rightarrow \gamma^*}$ with RG improvement at NLL accuracy

$$\begin{aligned}
F_V^{B \rightarrow \gamma^*}(n \cdot p, \bar{n} \cdot p) &= \hat{F}_A^{B \rightarrow \gamma^*}(n \cdot p, \bar{n} \cdot p) \\
&= \frac{Q_u m_B}{n \cdot p} \left[U_2(n \cdot p, \mu_{h2}, \mu) \tilde{f}_B(\mu_{h2}) \right] [U_1(n \cdot p, \mu_{h1}, \mu) C_\perp(n \cdot p, \mu_{h1})] \\
&\quad \times \int_0^\infty d\omega \frac{\phi_B^+(\omega, \mu)}{\omega - \bar{n} \cdot p - i0} J_\perp(n \cdot p, \bar{n} \cdot p, \omega, \mu) + \dots,
\end{aligned} \tag{55}$$

where the factorization scale needs to be chosen as a hard-collinear scale of order $\sqrt{\Lambda m_b}$, and μ_{h1} and μ_{h2} are the hard scales of order m_b .

3.6 Dispersion relation for the two-particle contribution at $\mathcal{O}(\alpha_s)$

It is now a straightforward task to derive the NLL resummation improved dispersion relations for the on-shell $B \rightarrow \gamma$ form factors. Employing the spectral representations of various convolution integrals displayed in Appendix A yields

$$\begin{aligned}
F_{V,2P}(n \cdot p) &= \hat{F}_{A,2P}(n \cdot p) \\
&= \frac{Q_u m_B}{n \cdot p} \left[U_2(n \cdot p, \mu_{h2}, \mu) \tilde{f}_B(\mu_{h2}) \right] [U_1(n \cdot p, \mu_{h1}, \mu) C_\perp(n \cdot p, \mu_{h1})] \\
&\quad \times \left\{ \int_0^\infty d\omega \frac{\phi_B^+(\omega, \mu)}{\omega} J_\perp(n \cdot p, 0, \omega, \mu) \right. \\
&\quad \left. + \int_0^{\omega_s} d\omega' \left[\frac{n \cdot p}{m_\rho^2} \text{Exp} \left[\frac{m_\rho^2 - \omega' n \cdot p}{n \cdot p \omega_M} \right] - \frac{1}{\omega'} \right] \phi_{B,\text{eff}}^+(\omega', \mu) \right\}, \\
&\equiv F_{V,2P}^{\text{LP}}(n \cdot p) + F_{V,2P}^{\text{NLP}}(n \cdot p),
\end{aligned} \tag{56}$$

where $F_{V,2P}^{\text{LP}}$ and $F_{V,2P}^{\text{NLP}}$ are defined by keeping only the first and the second terms in the bracket, respectively. In addition, the effective “distribution amplitude” $\phi_{B,\text{eff}}^+(\omega', \mu)$

$$\begin{aligned}
\phi_{B,\text{eff}}^+(\omega', \mu) &= \phi_B^+(\omega', \mu) + \frac{\alpha_s(\mu) C_F}{4\pi} \left\{ \int_0^{\omega'} d\omega \left[\frac{2}{\omega - \omega'} \ln \frac{\mu^2}{n \cdot p (\omega' - \omega)} \right]_\oplus \phi_B^+(\omega, \mu) \right. \\
&\quad \left. - \omega' \int_0^{\omega'} d\omega \left[\frac{1}{\omega - \omega'} \ln \frac{\omega' - \omega}{\omega} \right]_\oplus \frac{\phi_B^+(\omega', \mu)}{\omega} \right. \\
&\quad \left. + \frac{\omega'}{2} \int_0^\infty d\omega \left[\ln^2 \left| \frac{\omega - \omega'}{\omega'} \right| \right] \frac{d}{d\omega} \frac{\phi_B^+(\omega, \mu)}{\omega} \right. \\
&\quad \left. - \int_{\omega'}^\infty d\omega \left[\ln \frac{\mu^2}{n \cdot p \omega'} - \frac{\pi^2}{2} - 1 \right] \frac{d}{d\omega} \phi_B^+(\omega, \mu) \right. \\
&\quad \left. + \omega' \int_{\omega'}^\infty d\omega \left[\ln \frac{\mu^2}{n \cdot p \omega'} \ln \frac{\omega - \omega'}{\omega'} - \frac{1}{2} \ln^2 \frac{\mu^2}{n \cdot p (\omega - \omega')} + \frac{1}{2} \ln^2 \frac{\mu^2}{n \cdot p \omega'} \right] \right\}
\end{aligned}$$

$$+ 3 \ln \frac{\omega - \omega'}{\omega'} - \frac{2\pi^2}{3} \left] \frac{d}{d\omega} \frac{\phi_B^+(\omega, \mu)}{\omega} \right\}. \quad (57)$$

is introduced to absorb the next-to-leading-order (NLO) hard-collinear correction to the general $B \rightarrow \gamma^*$ transition form factors. It is evident that $F_{V,2P}^{\text{LP}}$ corresponds to the leading-power contribution to the on-shell $B \rightarrow \gamma$ form factors computed from QCD factorization and the corresponding convolution integral can be expressed in terms of the moments of the B -meson DA as [5]:

$$\begin{aligned} & \int_0^\infty d\omega \frac{\phi_B^+(\omega, \mu)}{\omega} J_\perp(n \cdot p, 0, \omega, \mu) \\ &= \lambda_B^{-1}(\mu) \left\{ 1 + \frac{\alpha_s(\mu) C_F}{4\pi} \left[\sigma_2(\mu) + 2 \ln \frac{\mu^2}{n \cdot p \mu_0} \sigma_1(\mu) + \ln^2 \frac{\mu^2}{n \cdot p \mu_0} - \frac{\pi^2}{6} - 1 \right] \right\}. \end{aligned} \quad (58)$$

Here, a hadronic reference scale $\mu_0 = 1 \text{ GeV}$ is introduced in the definition of the inverse-logarithmic moments, in contrast to [26], to avoid the appearance of a parametrically large logarithm due to the scale evolution of $\sigma_n(\mu)$ [5].

Several comments on the nonperturbative modification of the spectral function shown in the second term in the bracket of (56) are in order.

- In light of the power counting rule (26) and the scaling $\omega \sim \Lambda$ due to the canonical behaviour of the B -meson DA $\phi_B^+(\omega, \mu)$, one can readily identify that the logarithmic terms $\ln^2 \left| \frac{\omega - \omega'}{\omega'} \right|$ and $\ln \left(\frac{\omega - \omega'}{\omega'} \right)$ involved in (57) need to be counted as $\ln^2 \left(\frac{n \cdot p}{\Lambda} \right)$ and $\ln \left(\frac{n \cdot p}{\Lambda} \right)$ in the heavy quark limit. The appearance of such large logarithms can be traced back to the continuum subtraction in the construction of QCD sum rules for the end-point contribution to the $B \rightarrow \gamma$ form factors, with the aid of the parton-hadron duality approximation. This observation appears to indicate that the “hadronic” photon contribution to the $B \rightarrow \gamma \ell \nu$ amplitude suffers from rapidity divergences in QCD factorization, which are regularized by the nonperturbative parameter ω_M in the sum rule approach.
- In the absence of a detailed analysis of the subleading form factor $\xi(E_\gamma)$ in QCD [5], the precise relation between the end-point contribution computed from the hadronic dispersion relations and $\xi(E_\gamma)$ cannot be established in a model-independent way. It is rather plausible that adding up the symmetry-conserving form factor $\xi(E_\gamma)$ and the soft two-particle correction together would yield double counting of quark-gluon and hadron degrees of freedom.

4 Three-particle subleading power contribution

The purpose of this section is to compute the higher twist contributions to the on-shell $B \rightarrow \gamma$ transition form factors from the three-particle B -meson DAs at tree level. Following the main idea of the dispersion approach discussed in Section 2, we need to establish the factorization formula for the three-particle contribution to the generalized $B \rightarrow \gamma^*$ form factors at leading order in α_s . This amounts to evaluating the subleading power contribution (compared with

$$\begin{aligned}
&= \frac{\tilde{f}_B(\mu) m_B}{4} \int_0^\infty d\omega \int_0^\infty d\xi e^{-i(\omega+u\xi)v \cdot x} \left[(1 + \not{x}) \left\{ (v_\lambda \gamma_\rho - v_\rho \gamma_\lambda) [\Psi_A(\omega, \xi) - \Psi_V(\omega, \xi)] \right. \right. \\
&\quad \left. \left. - i \sigma_{\lambda\rho} \Psi_V(\omega, \xi) - \frac{x_\lambda v_\rho - x_\rho v_\lambda}{v \cdot x} X_A(\omega, \xi) + \frac{x_\lambda \gamma_\rho - x_\rho \gamma_\lambda}{v \cdot x} Y_A(\omega, \xi) \right\} \gamma_5 \right]_{\beta\alpha}, \quad (63)
\end{aligned}$$

with the soft Wilson lines on the left-hand side omitted for brevity. The three-particle DAs Ψ_V , Ψ_A , X_A and Y_A depend on two light-cone variables $\omega = \bar{n} \cdot k_1$ and $\xi = \bar{n} \cdot k_2$, where k_1 and k_2 are the light-quark and gluon momenta inside the B -meson. In contrast to the two-particle B -meson DAs, model-independent properties of the three-particle DAs in QCD, including the RG evolution equations and the asymptotic behaviours for $\omega, \xi \gg \Lambda$, are poorly explored at present (see [30] for an exception).

The tree-level factorization formula for the three-particle contribution to the on-shell $B \rightarrow \gamma$ form factors can be readily constructed by setting $\bar{n} \cdot p \rightarrow 0$ in (60):

$$\begin{aligned}
F_{V,3P}^{B \rightarrow \gamma}(n \cdot p) &= \hat{F}_{A,3P}^{B \rightarrow \gamma}(n \cdot p) \\
&= -\frac{Q_u \tilde{f}_B(\mu) m_B}{(n \cdot p)^2} \int_0^\infty d\omega \int_0^\infty d\xi \int_0^1 du \left\{ \frac{\rho_{3P}^{(2)}(u, \omega, \xi)}{[\omega + u\xi]^2} - \frac{\rho_{3P}^{(3)}(u, \omega, \xi)}{[\omega + u\xi]^3} \right\} \\
&= -\frac{Q_u \tilde{f}_B(\mu) m_B}{(n \cdot p)^2} \int_0^\infty d\omega \int_0^\infty d\xi \left\{ \frac{1}{\omega(\omega + \xi)} \Psi_V(\omega, \xi) \right. \\
&\quad \left. + \left[\frac{1}{\omega(\omega + \xi)} - \frac{2}{\xi(\omega + \xi)} + \frac{2}{\xi^2} \ln \frac{\omega + \xi}{\omega} \right] \Psi_A(\omega, \xi) + \frac{4\omega + \xi}{\omega^2(\omega + \xi)^2} \bar{X}_A(\omega, \xi) \right\}. \quad (64)
\end{aligned}$$

In light of the end-point behaviours of the three-particle B -meson DAs at $\omega, \xi \rightarrow 0$ from a QCD sum rule analysis [31]

$$\Psi_V(\omega, \xi) \sim \Psi_A(\omega, \xi) \sim \xi^2, \quad X_A(\omega, \xi) \sim \xi(2\omega - \xi), \quad Y_A(\omega, \xi) \sim \xi, \quad (65)$$

it is straightforward to verify that the convolution integral of the short-distance function with the B -meson DAs in (64) suffers from rapidity divergences as speculated in [6]. We therefore conclude that decomposing the three-particle contribution of the on-shell $B \rightarrow \gamma$ form factors into the factorizable effect computed from light-cone OPE and the nonperturbative modification as displayed in (24) and (25) cannot be justified, and instead one needs to employ the original dispersion expressions presented in (22) and (23).

Extracting the spectral function of (60) in the variable $\bar{n} \cdot p$ and substituting it into (22) and (23) give rise to the desired three-particle contribution to the $B \rightarrow \gamma$ form factors

$$\begin{aligned}
F_{V,3P}(n \cdot p) &= \hat{F}_{A,3P}(n \cdot p) \\
&= -\frac{Q_u \tilde{f}_B(\mu) m_B}{(n \cdot p)^2} \left\{ \frac{n \cdot p}{m_\rho^2} \text{Exp} \left[\frac{m_\rho^2}{n \cdot p \omega_M} \right] I_{3P}^I(\omega_s, \omega_M) + I_{3P}^{II}(\omega_s, \omega_M) \right\}, \quad (66)
\end{aligned}$$

where the coefficient functions entering (66) are

$$I_{3P}^I(\omega_s, \omega_M)$$

$$\begin{aligned}
&= \int_0^{\omega_s} d\omega \int_{\omega_s-\omega}^{\infty} \frac{d\xi}{\xi} e^{-\omega_s/\omega_M} \left[\rho_{3P}^{(2)}(u, \omega, \xi) - \frac{1}{2} \frac{d}{d\omega} \rho_{3P}^{(3)}(u, \omega, \xi) - \frac{\rho_{3P}^{(3)}(u, \omega, \xi)}{2\omega_M} \right] \Big|_{u=\frac{\omega_s-\omega}{\xi}} \\
&\quad + \int_0^{\omega_s} d\omega' \int_0^{\omega'} d\omega \int_{\omega'-\omega}^{\infty} \frac{d\xi}{\xi} e^{-\omega'/\omega_M} \frac{1}{\omega_M} \left[\rho_{3P}^{(2)}(u, \omega, \xi) - \frac{\rho_{3P}^{(3)}(u, \omega, \xi)}{2\omega_M} \right] \Big|_{u=\frac{\omega'-\omega}{\xi}}, \quad (67)
\end{aligned}$$

$$\begin{aligned}
&I_{3P}^{\text{II}}(\omega_s, \omega_M) \\
&= - \int_0^{\omega_s} d\omega \int_{\omega_s-\omega}^{\infty} \frac{d\xi}{\xi} \frac{1}{\omega_s} \left[\rho_{3P}^{(2)}(u, \omega, \xi) - \frac{1}{2} \frac{d}{d\omega} \rho_{3P}^{(3)}(u, \omega, \xi) - \frac{\rho_{3P}^{(3)}(u, \omega, \xi)}{2\omega_M} \right] \Big|_{u=\frac{\omega_s-\omega}{\xi}} \\
&\quad + \int_{\omega_s}^{\infty} d\omega' \int_0^{\omega'} d\omega \int_{\omega'-\omega}^{\infty} \frac{d\xi}{\xi} \frac{1}{(\omega')^2} \left[\rho_{3P}^{(2)}(u, \omega, \xi) - \frac{\rho_{3P}^{(3)}(u, \omega, \xi)}{2\omega_M} \right] \Big|_{u=\frac{\omega'-\omega}{\xi}}. \quad (68)
\end{aligned}$$

Employing the canonical behaviours of the three-particle B -meson DAs and the power counting rule (26) for the sum rule parameters leads to

$$I_{3P}^{\text{I}}(\omega_s, \omega_M) \sim \mathcal{O}(\Lambda^2/m_b), \quad I_{3P}^{\text{II}}(\omega_s, \omega_M) \sim \mathcal{O}(1), \quad (69)$$

which implies that both the “hard” and “soft” contributions to the $B \rightarrow \gamma$ form factors from the three-particle B -meson DAs scale as $(\Lambda/m_b)^{3/2}$ in the heavy quark limit, in contrast to the two-particle “hard” and “soft” contributions discussed before. Such observation can be also inferred from the violation of QCD factorization for the three-particle contribution to the form factors $F_V(n \cdot p)$ and $\hat{F}_A(n \cdot p)$, due to the rapidity divergences, indicating that the intuitive correspondence between the power expansion and the dynamical twist expansion can be spoiled by the soft corrections [16].

Adding up different pieces together, we obtain the final expressions for the on-shell $B \rightarrow \gamma$ form factors in the dispersion approach

$$F_V(n \cdot p) = F_{V,2P}(n \cdot p) + F_{V,3P}(n \cdot p) + F_{V,NLP}^{\text{LC}}(n \cdot p), \quad (70)$$

$$\hat{F}_A(n \cdot p) = \hat{F}_{A,2P}(n \cdot p) + \hat{F}_{A,3P}(n \cdot p) + \hat{F}_{A,NLP}^{\text{LC}}(n \cdot p), \quad (71)$$

where the manifest expressions of individual terms on the right-hand side of (70) and (71) are given by (56), (66) and (11), respectively. The following comments on the structures of the form factors $F_V(n \cdot p)$ and $\hat{F}_A(n \cdot p)$ displayed in (70) and (71) can be made.

- The symmetry-violating contribution to the on-shell $B \rightarrow \gamma$ form factors comes solely from the local subleading power corrections as indicated by $F_{V,NLP}^{\text{LC}}$ and $\hat{F}_{A,NLP}^{\text{LC}}$. The non-local subleading power contributions from the end-point region preserve the symmetry relation of F_V and \hat{F}_A due to the helicity conservation, in support of a similar observation made in [5] applying the QCD factorization approach.
- Despite of the fact that the leading-power contribution to the generalized $B \rightarrow \gamma^*$ form factors originates from the two-particle B -meson DA $\phi_B^+(\omega, \mu)$, the end-point (“soft”)

contributions to the on-shell $B \rightarrow \gamma$ form factors from both the two-particle and three-particle DAs contribute at the same power in the heavy-quark expansion. Following the arguments in [16], yet higher-twist corrections from the four-particle B -meson DAs would also generate the subleading power contribution suppressed by one power of Λ/m_b , when compared with the leading-twist contribution. We will leave a transparent demonstration of this interesting pattern for a future work, by including the two-gluon field strength terms and the covariant derivative of the $G^{\mu\nu}$ terms in the light-cone expansion of the massless-quark propagator in the background gluon field.

5 Numerical analysis

We are now in a position to explore the phenomenological consequence of the subleading power corrections to the $B \rightarrow \gamma$ form factors computed from the dispersion approach. In order to perform the numerical analysis of the newly derived expressions for $F_V(n \cdot p)$ and $\hat{F}_A(n \cdot p)$ in (70) and (71), we will proceed by specifying the nonperturbative models for the two-particle and three-particle DAs of the B -meson, determining the sum rule parameters and setting the hard and hard-collinear scales. Taking advantage of the new measurements of the partial branching fractions of $B \rightarrow \gamma \ell \nu$ from the Belle Collaboration [32], theory constraints of the inverse moment of the leading-twist DA $\phi_B^+(\omega, \mu)$ will be further addressed with the updated predictions for the $B \rightarrow \gamma$ form factors presented above.

5.1 Theory input parameters

Following [6], we will consider two models of the two-particle B -meson DA $\phi_B^+(\omega, \mu_0)$ motivated from the QCD sum rule analysis at tree level [20] and at NLO [26]

$$\phi_{B,I}^+(\omega, \mu_0) = \frac{\omega}{\omega_0^2} e^{-\omega/\omega_0}, \quad (72)$$

$$\phi_{B,II}^+(\omega, \mu_0) = \frac{1}{4\pi\omega_0} \frac{k}{k^2 + 1} \left[\frac{1}{k^2 + 1} - \frac{2(\sigma_1(\mu_0) - 1)}{\pi^2} \ln k \right], \quad k = \frac{\omega}{1 \text{ GeV}}, \quad (73)$$

where the shape parameter $\omega_0 = \lambda_B(\mu_0)$. As emphasized in [11], the above models can only serve as a reasonable description of $\phi_B^+(\omega, \mu_0)$ at small ω and they could not reproduce the model-independent behaviour at large ω predicted from perturbative QCD. Since the dominant contributions to the $B \rightarrow \gamma$ form factors come from the small ω region according to the power counting analysis, we will not improve the above models for the B -meson DA $\phi_B^+(\omega, \mu_0)$ by implementing the perturbative constraints as discussed in [33]. In particular, the leading power contribution to the on-shell $B \rightarrow \gamma$ form factors is insensitive to precise shape of $\phi_B^+(\omega, \mu_0)$ at small ω , and only depends on the inverse-logarithmic moments as shown in (58). Applying the one-loop evolution equation of $\phi_B^+(\omega, \mu)$ in (48) leads to [5]

$$\frac{\lambda_B(\mu_0)}{\lambda_B(\mu)} = 1 + \frac{\alpha_s(\mu_0) C_F}{4\pi} \ln \frac{\mu}{\mu_0} \left[2 - 2 \ln \frac{\mu}{\mu_0} - 4 \sigma_1(\mu_0) \right] + \mathcal{O}(\alpha_s^2). \quad (74)$$

For the inverse-logarithmic moments σ_1 and σ_2 , we will take $\sigma_1(\mu_0) = 1.5 \pm 1$ and $\sigma_2(\mu_0) = 3 \pm 2$ from [5], and the scale evolution effect of these parameters is not needed for the evaluation of the leading power contribution to the $B \rightarrow \gamma$ form factors at NLL.

For the three-particle B -meson DAs, we adopt an exponential model in consistent with the small ω, ξ behaviour from the tree-level QCD sum rule analysis [31]

$$\begin{aligned}\Psi_V(\omega, \xi, \mu_0) &= \Psi_A(\omega, \xi, \mu_0) = \frac{\lambda_E^2}{6\omega_0^4} \xi^2 e^{-(\omega+\xi)/\omega_0}, \\ X_A(\omega, \xi, \mu_0) &= \frac{\lambda_E^2}{6\omega_0^4} \xi (2\omega - \xi) e^{-(\omega+\xi)/\omega_0}, \\ Y_A(\omega, \xi, \mu_0) &= -\frac{\lambda_E^2}{24\omega_0^4} \xi (7\omega_0 - 13\omega + 3\xi) e^{-(\omega+\xi)/\omega_0},\end{aligned}\tag{75}$$

where the normalization parameter computed from QCD sum rules including the higher-order perturbative and nonperturbative effects is determined to be $\lambda_E^2(\mu_0) = (0.03 \pm 0.02) \text{ GeV}^2$ [34]. It needs to point out that we neglect the small correction due to the difference $(\Psi_A - \Psi_V) \sim (\lambda_E^2 - \lambda_H^2) \omega \xi^2$ which can be extracted from the NLO QCD correction to the sum rules for the three-particle DAs derived in [31], and the normalization coefficients in front of the DAs X_A and Y_A can also differ from λ_E^2 in general.

Now we turn to the determination of the Borel parameter ω_M and the duality-threshold parameter ω_s entering the expressions for $F_{V,2P}$ and $F_{V,3P}$. The general procedure to choose the sum rule parameters satisfying with the power counting rule (26) has been discussed in [11], and repeating the same strategies gives rise to the following intervals

$$M^2 \equiv n \cdot p \omega_M = (1.25 \pm 0.25) \text{ GeV}^2, \quad s_0 \equiv n \cdot p \omega_s = (1.50 \pm 0.20) \text{ GeV}^2, \tag{76}$$

in agreement with the values used for the LCSR for the $\gamma^* \rightarrow \pi\gamma$ form factor [16]. Note that the effective threshold ω_s in the dispersion expressions for the $B \rightarrow \gamma$ form factors should be compared to that adopted in the two-point sum rules for the ρ -meson channel [31].

The HQET decay constant of the B -meson $\tilde{f}_B(\mu)$ will be traded into the QCD decay constant f_B with the matching equation (15), which will be computed from the two-point QCD sum rules including $\mathcal{O}(\alpha_s)$ corrections to the perturbative contribution and the quark-gluon condensate operator contributions up to dimension-6 [35]. We will take the same intervals of the Borel mass and the threshold parameter

$$\overline{M}^2 = (5.0 \pm 1.0) \text{ GeV}^2, \quad \bar{s}_0 = (35.6_{-0.9}^{+2.1}) \text{ GeV}^2 \tag{77}$$

as adopted in [11, 35]. For the hard scales involved in the hard matching coefficients, we will choose $m_b/2 \leq \mu_{h1} = \mu_{h2} \leq 2m_b$ with the default value $\mu_{h1} = \mu_{h2} = m_b$. The factorization scale μ will be varied in the interval $1 \text{ GeV} \leq \mu \leq 2 \text{ GeV}$ around the central value 1.5 GeV . Furthermore, we will use the values of the bottom-quark mass in the $\overline{\text{MS}}$ scheme $\overline{m}_b(\overline{m}_b) = (4.193_{-0.035}^{+0.022}) \text{ GeV}$ determined from non-relativistic sum rules [36].

5.2 Predictions for the $B \rightarrow \gamma$ form factors

Now we are ready to investigate the numerical impact of the subleading power contributions from the two-particle and three-particle B -meson DAs on the $B \rightarrow \gamma$ form factors. To develop a transparent understanding of the newly calculated corrections in this work, we display the photon-energy dependence of the leading power two-particle contribution, the subleading power two-particle and three-particle corrections as well as the power suppressed local contribution in figure 4, where we take $\phi_{B,I}^+(\omega, \mu_0)$ as a default model with $\lambda_B(\mu_0) = 354_{-30}^{+38}$ MeV determined from [11]. One can readily find that, with the adopted value of $\lambda_B(\mu_0)$, the subleading power two particle contribution $F_{V,2P}^{\text{NLP,NLL}}(n \cdot p)$ including the NLL resummation effect can decrease the leading-power prediction for the form factor $F_V(n \cdot p)$ by approximately $(10 \sim 30)\%$ in the kinematic region $n \cdot p \in [2 \text{ GeV}, m_B]$; while the power suppressed correction from the three-particle B -meson DAs at tree level only induce a minor impact on the theory prediction of $F_V(n \cdot p)$ and numerically $\mathcal{O}(1\%)$. We also find that perturbative QCD corrections to the “soft” two-particle contribution can shift the tree-level prediction $F_{V,2P}^{\text{NLP,LL}}$ by an amount of $(10 \sim 20)\%$ with the default theory inputs. We are therefore led to conclude that the power suppressed corrections to the $B \rightarrow \gamma$ form factors are dominated by the soft two-particle contribution at tree level with the default model of B -meson DAs.

Keeping in mind that we aim at deriving the theory bound for the inverse moment $\lambda_B(\mu_0)$ of the B -meson DA $\phi_B^+(\omega, \mu_0)$ with the experimental data of the partial branching fractions of $B \rightarrow \gamma \ell \nu$, it is of interest to investigate the λ_B dependence of the subleading power corrections to the $B \rightarrow \gamma$ form factors. As can be observed from figure 5, the power suppressed two-particle contribution $F_{V,2P}^{\text{NLP,NLL}}$ decreases rapidly for $\lambda_B \leq 150$ MeV and it leads to a rather sizeable correction to the leading power prediction of the vector $B \rightarrow \gamma$ form factor $F_{V,2P}^{\text{LP,NLL}}$ for a reference value $\lambda_B(\mu_0) = 100$ MeV: $\mathcal{O}(45\%)$ at $n \cdot p = m_B$ and $\mathcal{O}(100\%)$ at $n \cdot p = 2 \text{ GeV}$. Also, we find that the NLL resummation improved perturbative correction to the soft two-particle contribution becomes more important numerically with the decrease of $\lambda_B(\mu_0)$: approximately $(20 \sim 40)\%$ for $n \cdot p \in [2 \text{ GeV}, m_B]$ with $\lambda_B(\mu_0) = 100$ MeV. We can readily conclude the “soft” two-particle contribution to the on-shell $B \rightarrow \gamma$ form factors is not effectively suppressed numerically at small $\lambda_B(\mu_0)$ as expected from the power counting analysis in the heavy quark limit. Moreover, we observe that the subleading power three-particle correction to the $B \rightarrow \gamma$ form factors is still insignificant even at $\lambda_B(\mu_0) = 100$ MeV, approximately $\mathcal{O}(1\%)$, compared with the factorizable two-particle contribution.

To understand such “anomalous” feature of the subleading power two-particle correction, we first recall that the power counting scheme established above makes use of the canonical behaviour of the B -meson DA $\phi_B^+(\omega, \mu_0)$ [37]

$$\phi_B^+(\omega, \mu_0) \sim \begin{cases} 1/\Lambda; & \omega \sim \Lambda \\ 0; & \omega \gg \Lambda \end{cases}, \quad (78)$$

which implies that the inverse moment $\lambda_B(\mu_0)$ scales as Λ in consistent with the generic scaling of the light-quark momentum in the B -meson. However, it would be more appropriate to count the scaling of the inverse moment as $\lambda_B(\mu_0) \sim \Lambda^2/m_b$ for $\lambda_B(\mu_0) \leq 100$ MeV in the heavy

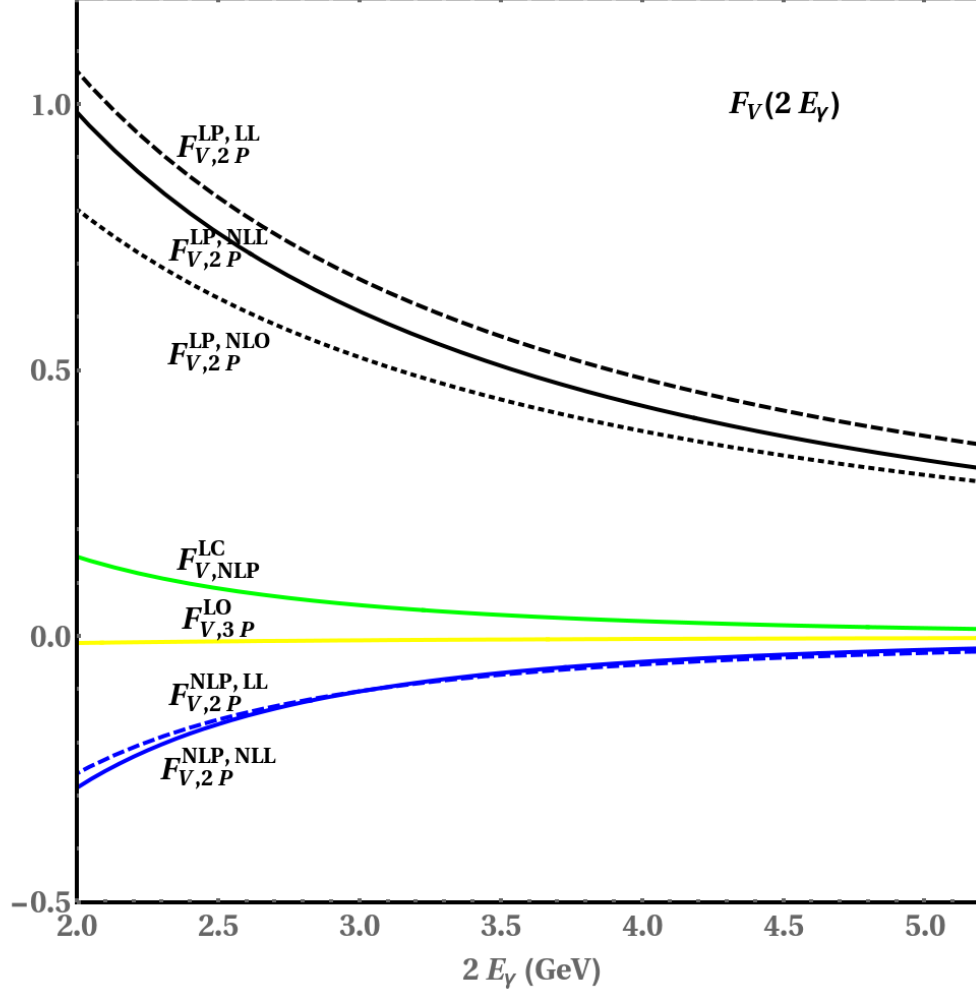


Figure 4: The photon-energy dependence of various contributions to the form factor $F_V(2 E_\gamma)$, with the exponential model of $\phi_B^+(\omega, \mu_0)$ and the inverse moment $\lambda_B(\mu_0) = 354 \text{ MeV}$ determined in [11]. The separate contributions correspond to the leading power two-particle effect at leading logarithmic (LL) accuracy ($F_{V,2P}^{\text{LP,LL}}$, dashed black), at NLO ($F_{V,2P}^{\text{LP,NLO}}$, dotted black), and at NLL ($F_{V,2P}^{\text{LP,NLL}}$, solid black); the subleading power two-particle correction at LL ($F_{V,2P}^{\text{NLP,LL}}$, dashed blue), and at NLL ($F_{V,2P}^{\text{NLP,NLL}}$, solid blue); the subleading power three-particle correction at LO ($F_{V,3P}^{\text{LO}}$, solid yellow); and the power suppressed local effect at tree level ($F_{V,NLP}^{\text{LC}}$, solid green).

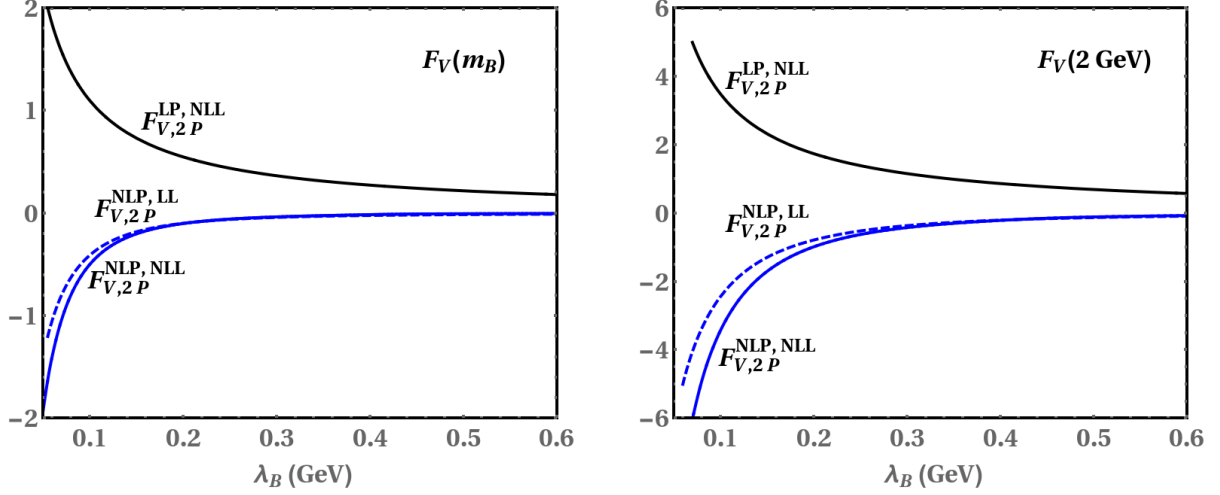


Figure 5: Dependence of the leading and subleading power two-particle contributions to the form factor $F_V(n \cdot p)$ on the inverse moment $\lambda_B(\mu_0)$ at zero momentum transfer (left panel) and at $n \cdot p = 2 \text{ GeV}$ (right panel). Same conventions as in figure 4.

quark limit. Applying this new power counting scheme leads to

$$F_{V,2P}^{\text{LP}} \sim F_{V,2P}^{\text{NLP}} \sim \left(\frac{m_b}{\Lambda}\right)^{1/2}, \quad \text{for } \lambda_B(\mu_0) \sim \Lambda^2/m_b, \quad (79)$$

which indicates that the “soft” two-particle contribution to the $B \rightarrow \gamma$ form factors is of the same power in the heavy quark expansion as the factorizable effect computed from the QCD factorization approach. To validate the leading-power factorization formula for the generalized $B \rightarrow \gamma^*$ form factors (55), we will therefore only focus on the inverse moment region $\lambda_B(\mu_0) \geq 200 \text{ MeV}$ in accordance with the power counting $\lambda_B(\mu_0) \sim \Lambda$ in the following analysis, which implies the desired power counting rule for the “soft” two-particle correction

$$F_{V,2P}^{\text{LP}} \sim \left(\frac{\Lambda}{m_b}\right)^{1/2}, \quad F_{V,2P}^{\text{NLP}} \sim \left(\frac{\Lambda}{m_b}\right)^{3/2}, \quad \text{for } \lambda_B(\mu_0) \sim \Lambda. \quad (80)$$

We turn to investigate phenomenological impacts of the model dependence of $\phi_B^+(\omega, \mu)$ on the theoretical predictions of the $B \rightarrow \gamma$ form factors. It is evident from figure 6 that the form factors F_V and F_A are insensitive to the specific model of the B -meson DA $\phi_B^+(\omega, \mu)$ for a large value of $\lambda_B(\mu_0)$. This can be readily understood from the fact that the leading power contribution to the $B \rightarrow \gamma$ form factors is determined by the inverse-logarithmic moments completely and the subleading power two-particle and three-particle corrections are both parametrically and numerically suppressed compared with the leading power effect at large $\lambda_B(\mu_0)$. The distinct predictions of the $B \rightarrow \gamma$ form factors from different nonperturbative models of $\phi_B^+(\omega, \mu)$ at small $\lambda_B(\mu_0)$, displayed in figure 6, imply that soft (end-point) contributions to the form factors F_V and F_A are both numerically sizable and heavily dependent on the precise shape of the $\phi_B^+(\omega, \mu)$ at small ω , in agreement with a similar observation for the $B \rightarrow \pi$ form factors

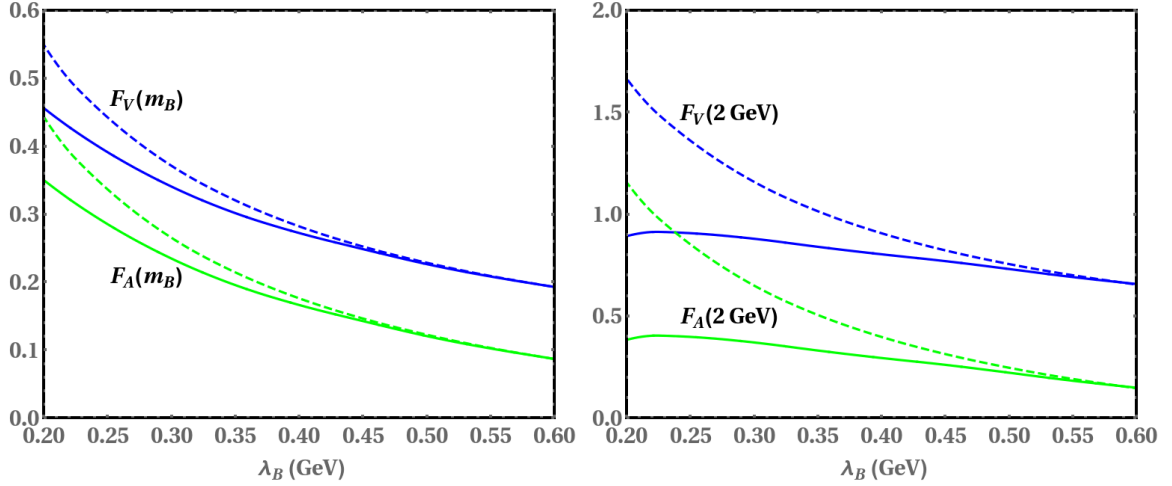


Figure 6: Dependence of the form factors $F_V(n \cdot p)$ and $F_A(n \cdot p)$ on the specific model for the B -meson DA $\phi_B^+(\omega, \mu)$ at $n \cdot p = m_B$ (left panel) and at $n \cdot p = 2 \text{ GeV}$ (right panel). The solid and dashed blue (green) curves indicate the theory predictions of F_V (F_A) from the first and second models of ϕ_B^+ displayed in (72) and (73), respectively.

[11]. In particular, the resulting discrepancies for the form factor predictions due to different parameterizations of $\phi_B^+(\omega, \mu)$ will be further enhanced at $n \cdot p = 2 \text{ GeV}$ due to the raise of power suppressed corrections.

Now we proceed to perform a numerical comparison of the power suppressed two-particle and three-particle corrections to the $B \rightarrow \gamma$ form factors $F_{V,2P}^{\text{NLP,NLL}} + F_{V,3P}^{\text{LO}}$, computed from the dispersion approach, and the subleading power symmetry-conserving form factor $\xi(2 E_\gamma)$ introduced in [5]. In the absence of a detailed analysis of $\xi(2 E_\gamma)$, a simple model in compatible with the power counting analysis in the heavy quark limit

$$\xi(2 E_\gamma) = c \frac{f_B}{2 E_\gamma} \quad (81)$$

was proposed in [5], assuming the same E_γ dependence as the leading power contribution $F_{V,2P}^{\text{LP}}(2 E_\gamma)$. One can readily conclude from figure 7 that the nonperturbative parameter c needs to be significantly larger than one at $E_\gamma \simeq 1 \text{ GeV}$ so that $\xi(2 E_\gamma)$ can match the non-local subleading power contributions to the $B \rightarrow \gamma$ form factors numerically, confirming the observation made in [6]. In addition, we observe that the photon-energy dependence of the soft contribution $F_{V,2P}^{\text{NLP}} + F_{V,3P}$ cannot be well described by the simple model (81) particularly for $E_\gamma \leq 1.5 \text{ GeV}$.

We further present the main theory predictions for the photon-energy dependence of the $B \rightarrow \gamma$ form factors in figure 8, taking into account the newly computed power suppressed two-particle and three-particle contributions $F_{V,2P}^{\text{NLP}} + F_{V,3P}$. Several comments on the numerical results obtained above are in order.

- The dominant theory uncertainties arise from the factorization scale μ , the inverse-logarithmic moments $\lambda_B(\mu_0)$, $\sigma_1(\mu_0)$ and $\sigma_2(\mu_0)$, as well as the model dependence of the

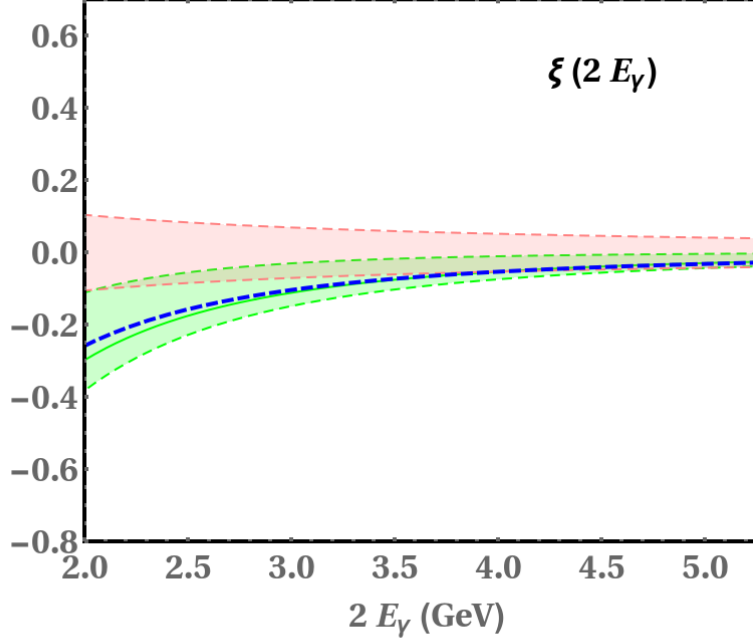


Figure 7: The non-local effect due to photon radiation off the up anti-quark parameterized by the subleading power form factor $\xi(2E_\gamma)$ (pink band) [5] compared with the sum of the power suppressed two-particle and three-particle corrections $F_{V,2P}^{\text{NLP,NLL}} + F_{V,3P}^{\text{LO}}$ computed from the dispersion approach (green band) with $\lambda_B(\mu_0) = 354 \text{ MeV}$ determined in [11]. The blue curve refers to the LL prediction for the soft two-particle contribution with the default choices of theory inputs.

B -meson DA $\phi_B^+(\omega, \mu_0)$. The strong sensitivity of the soft two-particle contribution to the precise shape of $\phi_B^+(\omega, \mu_0)$ at small ω is not unexpected by inspecting the analytical expression of $F_{V,2P}^{\text{NLP}}(n \cdot p)$ in (56).

- Since the subleading power two-particle and three-particle corrections to the $B \rightarrow \gamma$ form factors preserve the symmetry relation for the leading power contributions due to helicity conservation, the symmetry-breaking effect still originates from the subleading power local corrections with the current accuracy [5]

$$F_A(n \cdot p) - F_V(n \cdot p) = \frac{2f_B}{n \cdot p} \left[Q_\ell - \frac{Q_u m_B}{n \cdot p} - \frac{Q_b m_B}{m_b} \right] + \mathcal{O}(\alpha_s), \quad (82)$$

dependent only on the B -meson decay constant f_B . This also explains why the form factor difference only suffers from a very small uncertainty as displayed in figure 8, albeit with the large theory uncertainty for the individual form factor.

- Since the photon-energy dependence of the form factors F_V and F_A is controlled by the nearest poles in the vector and axial-vector ($b\bar{u}$) channels, the vector form factor F_V grows faster than F_A with the increase of q^2 (i.e., with the decrease of E_γ) in compatible with the prediction presented in figure 8.

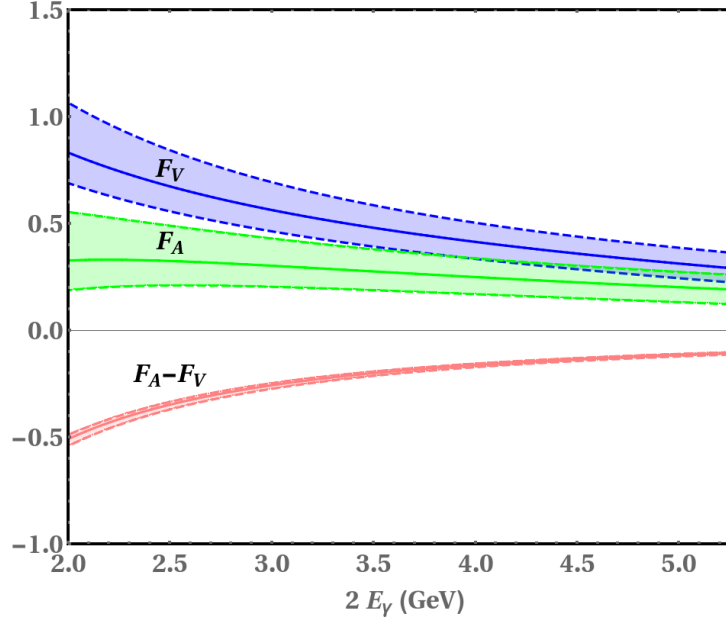


Figure 8: The photon-energy dependence of the form factors $F_V(2 E_\gamma)$ and $F_A(2 E_\gamma)$ as well as their difference with $\lambda_B(\mu_0) = 354 \text{ MeV}$. The theory uncertainties from variations of different input parameters are added in quadrature.

Having at our disposal the theory predictions for the $B \rightarrow \gamma$ form factors, we turn to explore the theory constraint on $\lambda_B(\mu_0)$ from the partial branching fractions of $B \rightarrow \gamma \ell \nu$. Since the factorization formula for the decay amplitude $\mathcal{A}(B^- \rightarrow \gamma \ell \nu)$ was established with the power counting scheme $n \cdot p \equiv 2 E_\gamma \sim \mathcal{O}(m_b)$, the phase-space cut on the photon energy needs to be introduced in the definition of the integrated decay rate

$$\Delta \mathcal{BR}(E_{\text{cut}}) = \tau_B \int_{E_{\text{cut}}}^{m_B/2} dE_\gamma \frac{d\Gamma}{dE_\gamma} (B \rightarrow \gamma \ell \nu) , \quad (83)$$

in order to facilitate the comparison of the experimental measurements from the Belle Collaboration [32] and the theoretical predictions displayed in figure 9. The main observations can be summarized as follows.

- Employing the upper limit of the partial branching fraction with $E_{\text{cut}} = 1 \text{ GeV}$ from the Belle experiment $\Delta \mathcal{BR}(1 \text{ GeV}) < 3.5 \times 10^{-6}$, we find that no interesting bound on $\lambda_B(\mu_0)$ for the Grozin-Neubert model (72) can be deduced from the weak experiment limit, when the subleading power two-particle and three-particle corrections to the $B \rightarrow \gamma$ form factors are taken into account in the theory predictions. In contrast, applying the formulae for the transition form factors F_V and F_A computed from QCD factorization [5]

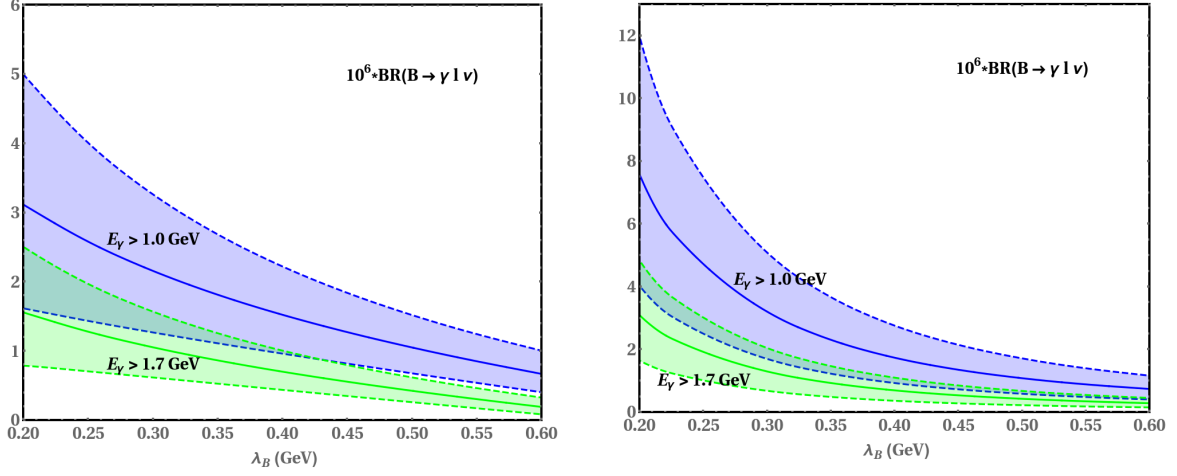


Figure 9: The inverse-moment $\lambda_B(\mu_0)$ dependence of the partial branching fractions of $\mathcal{BR}(B \rightarrow \gamma \ell \nu, E_\gamma \geq E_{\text{cut}})$ for $E_{\text{cut}} = 1 \text{ GeV}$ (blue band) and $E_{\text{cut}} = 1.7 \text{ GeV}$ (green band) with the model $\phi_{B,I}^+(\omega, \mu_0)$ based upon the Grozin-Neubert parametrization (left panel) and with the model $\phi_{B,II}^+(\omega, \mu_0)$ based upon the Braun-Ivanov-Korchensky parametrization (right panel).

directly yields a meaningful bound $\lambda_B(\mu_0) > 217 \text{ MeV}$. The discrepancy can be traced back to the rapidly growing soft two-particle contribution with the reduction of $\lambda_B(\mu_0)$ as presented in figure 5, which can induce a strong cancellation between the leading power contributions and the power suppressed effects. We are therefore led to conclude that the power suppressed two-particle and three-particle contributions computed in this work are indispensable to the extraction of the inverse moment $\lambda_B(\mu_0)$ from the radiative leptonic $B \rightarrow \gamma \ell \nu$ decay.

- Due to the apparent larger branching fractions of $B \rightarrow \gamma \ell \nu$ predicted from the model $\phi_{B,II}^+(\omega, \mu_0)$ in (73) at small $\lambda_B(\mu_0)$, the above-mentioned Belle limit yields a loose bound $\lambda_B(\mu_0) > 214 \text{ MeV}$. The strong sensitivity of the extracted bound of $\lambda_B(\mu_0)$ on the parametrization of the leading-twist B -meson DA can be understood from the model-dependence of $\phi_B^+(\omega, \mu)$ on predicting the $B \rightarrow \gamma$ form factors displayed in figure 6. Such model dependence in the evaluation of the $B \rightarrow \gamma$ form factors will be significantly reduced only for $\lambda_B(\mu_0) \geq 500 \text{ MeV}$ where the leading power contribution to the form factors F_V and F_A computed from QCD factorization approach also turns out to be numerically dominant. Precision measurements of the binned distribution of $B \rightarrow \gamma \ell \nu$ from the forthcoming Belle II experiment at KEK are expected to shed light on the information of $\phi_B^+(\omega, \mu)$ at small ω .

6 Conclusion and outlook

Applying the dispersion approach developed in the context of the pion-photon transition form factor, we computed perturbative QCD corrections to the subleading power soft two-particle contribution of the $B \rightarrow \gamma$ transition form factors, which cannot be addressed directly with the QCD factorization approach due to the breakdown of light-cone OPE in the end-point region. To achieve this goal, we first demonstrated QCD factorization for the generalized $B \rightarrow \gamma^*$ form factors with a hard-collinear photon at leading power in Λ/m_b using the diagrammatic factorization approach. Both the hard coefficient and jet function entering the factorization formulae for the $B \rightarrow \gamma^*$ form factors were determined at one loop explicitly based upon the method of regions. We further verified that the hard function C_\perp is consistent with the perturbative matching coefficient of the QCD weak current $\bar{u} \gamma_{\mu\perp} (1 - \gamma_5) b$ in SCET, and the hard-collinear function J_\perp reproduces the jet function involved in the factorization formulae for the on-shell $B \rightarrow \gamma$ form factors when setting $\bar{n} \cdot p \rightarrow 0$. Employing the RG evolution equations in the momentum space, we obtained the NLL resummation improved factorization formulae for the generalized $B \rightarrow \gamma^*$ form factors at leading power in Λ/m_b , which allows one to derive the expression for the soft two-particle correction to the $B \rightarrow \gamma$ form factors straightforwardly with the standard dispersion relation in the variable p^2 . We also mention in passing that the above-mentioned factorization formulae for the $B \rightarrow \gamma^*$ form factors can be also employed to construct the NLL sum rules for the $B \rightarrow \rho$ form factors at large recoil.

Along the same vein, we also constructed the factorization formula for the three-particle contribution to the generalized $B \rightarrow \gamma^*$ form factors at tree level. In accordance with the end-point behaviours of the three-particle B -meson DAs, we showed that QCD factorization for the three-particle contribution to the on-shell $B \rightarrow \gamma$ form factors is violated due to the rapidity divergences in the corresponding convolution integrals. Moreover, both the “soft” and “hard” three-particle corrections to the $B \rightarrow \gamma$ form factors were shown to contribute at the same power in Λ/m_b with the aid of the dispersion approach, in contrast to the two-particle counterparts. In particular, the newly computed subleading power two-particle and three-particle corrections turn out to preserve the symmetry relation of the leading power contribution to F_V and F_A as a consequence of the helicity conservation.

Having at hand the dispersion expressions for the $B \rightarrow \gamma$ form factors, we proceeded to explore the phenomenological impacts of the power suppressed two-particle and three-particle contributions in detail. Employing the nonperturbative models of the B -meson DA $\phi_B^\pm(\omega, \mu_0)$ motivated from the tree-level and the NLO QCD sum rule computations, we found that perturbative QCD corrections to the soft two-particle contribution can give rise to $(10 \sim 20)\%$ shift to the tree-level prediction at $\lambda_B(\mu_0) = 354 \text{ MeV}$, and the three-particle correction to the $B \rightarrow \gamma$ form factors at leading order in α_s was found to be of $\mathcal{O}(1\%)$ numerically with the exponential model of the three-particle DAs and with the same value of the inverse moment. However, the soft two-particle correction to the $B \rightarrow \gamma$ form factors can be significantly enhanced for $\lambda_B(\mu_0) \leq 150 \text{ MeV}$ and it yields a strong cancellation against the leading power contributions computed in QCD factorization. We further argued that the “anomalous” soft two-particle contribution at small $\lambda_B(\mu_0)$ can be understood from the power counting analysis of the analytical expression (56) with an appropriate scaling $\lambda_B \sim \Lambda^2/m_b$ in this regard. Numerically the subleading power two-particle and three-particle contributions to the $B \rightarrow \gamma$

form factors were evaluated to be considerably greater than the power suppressed symmetry-conserving form factor $\xi(2E_\gamma)$, estimated from the simple phenomenological model (81), at $E_\gamma \simeq 1$ GeV. Our main theory predictions for the form factors F_V and F_A including the subleading power contributions from the two-particle DA ϕ_B^+ at NLL and from the three-particle DAs at tree level were presented in figure 8. With the theory predictions for the $B \rightarrow \gamma$ form factors at hand, we proceeded with computing the integrated branching fractions of $B \rightarrow \gamma \ell \nu$ with the phase-space cut on the photon energy $E_\gamma \geq E_{\text{cut}}$. The theory constraint of the inverse moment λ_B derived from the recent Belle data on $\mathcal{BR}(B \rightarrow \gamma \ell \nu)$ was found to be sensitive to the specific model of ϕ_B^+ adopted in the evaluation of the form factors F_V and F_A , since the subleading power soft two-particle correction is not sufficiently suppressed numerically at small λ_B and dependent on the precise shape of ϕ_B^+ at small ω . Remarkably, no interesting bound on the inverse moment λ_B can be derived, with the model $\phi_{B,1}^+(\omega, \mu_0)$ in (72), from the inconclusive Belle measurement $\Delta\mathcal{BR}(1 \text{ GeV}) < 3.5 \times 10^{-6}$, when the subleading power two-particle and three-particle corrections are taken into account. In contrast, employing an alternative model based on the Braun-Ivanov-Korchemsky parametrization (73) would yield a weak bound $\lambda_B(\mu_0) > 214 \text{ MeV}$ from the Belle data, due to the substantially enhanced predictions for the branching fractions of $B \rightarrow \gamma \ell \nu$ at small $\lambda_B(\mu_0)$.

Exploring the strong interaction dynamics of the radiative leptonic $B \rightarrow \gamma \ell \nu$ decay beyond this work can be pursued in different directions. First, it would be of interest to investigate the factorization property of the subleading power form factor $\xi(2E_\gamma)$ in QCD, and then to build up the relation between the non-local subleading power corrections computed from the dispersion approach and $\xi(2E_\gamma)$ expressed in terms of the higher-twist B -meson DAs. Second, calculating the yet higher-twist corrections to the $B \rightarrow \gamma$ form factors from the four-particle B -meson DAs in the framework of the dispersion approach will be helpful to clarify whether they are indeed suppressed by one power of Λ/m_b due to the mismatch between the twist expansion and the power expansion, and to verify whether the non-local higher-twist contributions generate the symmetry-breaking effect between F_V and F_A as observed from the sum rule approach with the photon DAs. Third, extending the current analysis by computing perturbative corrections to the three-particle contributions of the generalized $B \rightarrow \gamma^*$ form factors will deepen our understanding towards QCD factorization for the subleading power contributions in exclusive B -meson decays, and more important, such computations will be essential to construct the NLL sum rules for $B \rightarrow \rho$ form factors even at leading power in Λ/m_b . To summarize, we believe that precision QCD calculations of the radiative $B \rightarrow \gamma \ell \nu$ decay are sufficiently interesting on both the conceptual and phenomenological aspects.

Acknowledgements

The author is grateful to Martin Beneke and Vladimir Braun for illuminating discussions, and to Vladimir Braun for valuable comments on the manuscript.

A Spectral representations

Here we collect the dispersion representations of various convolution integrals involved in the factorization formulae for the generalized $B \rightarrow \gamma^*$ form factors presented in (55). In particular, we confirm the following spectral representations by verifying the corresponding dispersion integrals manifestly.

$$\begin{aligned} & \frac{1}{\pi} \text{Im}_{\omega'} \int_0^\infty \frac{d\omega}{\omega - \omega' - i0} \ln^2 \frac{\mu^2}{n \cdot p (\omega - \omega')} \phi_B^+(\omega, \mu) \\ &= \int_0^\infty d\omega \left[\frac{2\theta(\omega' - \omega)}{\omega - \omega'} \ln \frac{\mu^2}{n \cdot p (\omega' - \omega)} \right]_\oplus \phi_B^+(\omega, \mu) + \left[\ln \frac{\mu^2}{n \cdot p \omega'} - \frac{\pi^2}{3} \right] \phi_B^+(\omega', \mu), \end{aligned} \quad (84)$$

$$\begin{aligned} & \frac{1}{\pi} \text{Im}_{\omega'} \int_0^\infty \frac{d\omega}{\omega - \omega' - i0} \frac{\omega'}{\omega} \ln \frac{\omega' - \omega}{\omega'} \ln \frac{\mu^2}{-n \cdot p \omega'} \phi_B^+(\omega, \mu) \\ &= -\frac{\omega'}{2} \left\{ \int_0^\infty d\omega \ln^2 \left| \frac{\omega - \omega'}{\omega'} \right| \frac{d}{d\omega} \frac{\phi_B^+(\omega', \mu)}{\omega} \right. \\ & \quad \left. + \int_{\omega'}^\infty d\omega \left[2 \ln \frac{\mu^2}{n \cdot p \omega'} \ln \frac{\omega - \omega'}{\omega'} - \pi^2 \right] \frac{d}{d\omega} \frac{\phi_B^+(\omega', \mu)}{\omega} \right\}, \end{aligned} \quad (85)$$

$$\begin{aligned} & \frac{1}{\pi} \text{Im}_{\omega'} \int_0^\infty \frac{d\omega}{\omega - \omega' - i0} \frac{\omega'}{\omega} \ln \frac{\omega' - \omega}{\omega'} \ln \frac{\mu^2}{n \cdot p (\omega - \omega')} \phi_B^+(\omega, \mu) \\ &= \omega' \left\{ \int_0^\infty d\omega \left[\frac{\theta(\omega' - \omega)}{\omega - \omega'} \ln \frac{\omega' - \omega}{\omega'} \right]_\oplus \frac{\phi_B^+(\omega', \mu)}{\omega} \right. \\ & \quad \left. + \frac{1}{2} \int_{\omega'}^\infty d\omega \left[\ln^2 \frac{\mu^2}{n \cdot p (\omega - \omega')} - \ln^2 \frac{\mu^2}{n \cdot p \omega'} + \frac{\pi^2}{3} \right] \frac{d}{d\omega} \frac{\phi_B^+(\omega', \mu)}{\omega} \right\}, \end{aligned} \quad (86)$$

$$\begin{aligned} & \frac{1}{\pi} \text{Im}_{\omega'} \int_0^\infty \frac{d\omega}{\omega - \omega' - i0} \frac{\omega'}{\omega} \ln \frac{\omega' - \omega}{\omega'} \phi_B^+(\omega, \mu) \\ &= -\omega' \int_{\omega'}^\infty d\omega \ln \frac{\omega - \omega'}{\omega'} \frac{d}{d\omega} \frac{\phi_B^+(\omega, \mu)}{\omega}. \end{aligned} \quad (87)$$

References

- [1] G. P. Korchemsky, D. Pirjol and T. M. Yan, Phys. Rev. D **61** (2000) 114510 [hep-ph/9911427].
- [2] S. Descotes-Genon and C. T. Sachrajda, Nucl. Phys. B **650** (2003) 356 [hep-ph/0209216].
- [3] E. Lunghi, D. Pirjol and D. Wyler, Nucl. Phys. B **649** (2003) 349 [hep-ph/0210091].
- [4] S. W. Bosch, R. J. Hill, B. O. Lange and M. Neubert, Phys. Rev. D **67** (2003) 094014 [hep-ph/0301123].

- [5] M. Beneke and J. Rohrwild, Eur. Phys. J. C **71** (2011) 1818 [arXiv:1110.3228 [hep-ph]].
- [6] V. M. Braun and A. Khodjamirian, Phys. Lett. B **718** (2013) 1014 [arXiv:1210.4453 [hep-ph]].
- [7] C. W. Bauer, S. Fleming, D. Pirjol and I. W. Stewart, Phys. Rev. D **63** (2001) 114020 [hep-ph/0011336].
- [8] C. W. Bauer, D. Pirjol and I. W. Stewart, Phys. Rev. D **65** (2002) 054022 [hep-ph/0109045].
- [9] M. Beneke, A. P. Chapovsky, M. Diehl and T. Feldmann, Nucl. Phys. B **643** (2002) 431 [hep-ph/0206152].
- [10] M. Beneke and V. A. Smirnov, Nucl. Phys. B **522** (1998) 321 [hep-ph/9711391].
- [11] Y. M. Wang and Y. L. Shen, Nucl. Phys. B **898** (2015) 563 [arXiv:1506.00667 [hep-ph]].
- [12] Y. M. Wang and Y. L. Shen, JHEP **1602** (2016) 179 [arXiv:1511.09036 [hep-ph]].
- [13] A. Khodjamirian, G. Stoll and D. Wyler, Phys. Lett. B **358** (1995) 129 [hep-ph/9506242].
- [14] G. Eilam, I. E. Halperin and R. R. Mendel, Phys. Lett. B **361** (1995) 137 [hep-ph/9506264].
- [15] P. Ball and E. Kou, JHEP **0304** (2003) 029 [hep-ph/0301135].
- [16] S. S. Agaev, V. M. Braun, N. Offen and F. A. Porkert, Phys. Rev. D **83** (2011) 054020 [arXiv:1012.4671 [hep-ph]].
- [17] B. Grinstein and D. Pirjol, Phys. Rev. D **62** (2000) 093002 [hep-ph/0002216].
- [18] A. Khodjamirian and D. Wyler, In “Gurzadyan, V.G. (ed.) et al.: From integrable models to gauge theories” 227-241 [hep-ph/0111249].
- [19] A. Khodjamirian, Eur. Phys. J. C **6** (1999) 477 [hep-ph/9712451].
- [20] A. G. Grozin and M. Neubert, Phys. Rev. D **55** (1997) 272 [hep-ph/9607366].
- [21] M. Beneke and T. Feldmann, Nucl. Phys. B **592** (2001) 3 [hep-ph/0008255].
- [22] M. Beneke and D. S. Yang, Nucl. Phys. B **736** (2006) 34 [hep-ph/0508250].
- [23] C. W. Bauer, S. Fleming and M. E. Luke, Phys. Rev. D **63** (2000) 014006 [hep-ph/0005275].
- [24] M. Beneke, Y. Kiyo and D. S. Yang, Nucl. Phys. B **692** (2004) 232 [hep-ph/0402241].
- [25] B. O. Lange and M. Neubert, Phys. Rev. Lett. **91** (2003) 102001 [hep-ph/0303082].

- [26] V. M. Braun, D. Y. Ivanov and G. P. Korchemsky, Phys. Rev. D **69** (2004) 034014 [hep-ph/0309330].
- [27] I. I. Balitsky and V. M. Braun, Nucl. Phys. B **311** (1989) 541.
- [28] H. Kawamura, J. Kodaira, C. F. Qiao and K. Tanaka, Phys. Lett. B **523** (2001) 111
Erratum: [Phys. Lett. B **536** (2002) 344] [hep-ph/0109181].
- [29] B. Geyer and O. Witzel, Phys. Rev. D **72** (2005) 034023 [hep-ph/0502239].
- [30] V. M. Braun, A. N. Manashov and N. Offen, Phys. Rev. D **92** (2015) 074044 [arXiv:1507.03445 [hep-ph]].
- [31] A. Khodjamirian, T. Mannel and N. Offen, Phys. Rev. D **75** (2007) 054013 [hep-ph/0611193].
- [32] A. Heller *et al.* [Belle Collaboration], Phys. Rev. D **91** (2015) 112009 [arXiv:1504.05831 [hep-ex]].
- [33] T. Feldmann, B. O. Lange and Y. M. Wang, Phys. Rev. D **89** (2014) 114001 [arXiv:1404.1343 [hep-ph]].
- [34] T. Nishikawa and K. Tanaka, Nucl. Phys. B **879** (2014) 110 [arXiv:1109.6786 [hep-ph]].
- [35] G. Duplancic, A. Khodjamirian, T. Mannel, B. Melic and N. Offen, JHEP **0804** (2008) 014 [arXiv:0801.1796 [hep-ph]].
- [36] M. Beneke, A. Maier, J. Piclum and T. Rauh, Nucl. Phys. B **891** (2015) 42 [arXiv:1411.3132 [hep-ph]].
- [37] M. Beneke, G. Buchalla, M. Neubert and C. T. Sachrajda, Nucl. Phys. B **591** (2000) 313 [hep-ph/0006124].